THE JOURNAL OF PHYSICAL CHEMISTRY A

Article

pubs.acs.org/JPCA

Experimental Benchmark Data and Systematic Evaluation of Two *a Posteriori*, Polarizable-Continuum Corrections for Vertical Excitation Energies in Solution

Jan-Michael Mewes,[†] Zhi-Qiang You,[‡] Michael Wormit,[†] Thomas Kriesche,[§] John M. Herbert,[‡] and Andreas Dreuw*[,†]

[†]Interdisciplinary Center for Scientific Computing, Ruprechts-Karls University, Im Neuenheimer Feld 368, 69120 Heidelberg, Germany

[‡]Department of Chemistry and Biochemistry, The Ohio State University, Columbus, Ohio 43210, United States

[§]Institute for Physical Chemistry, Ruprechts-Karls University, 69120 Heidelberg, Germany

Supporting Information

ABSTRACT: We report the implementation and evaluation of a perturbative, density-based correction scheme for vertical excitation energies calculated in the framework of a polarizable continuum model (PCM). Because the proposed first-order correction terms depend solely on the zeroth-order excited-state density, a transfer of the approach to any configuration interaction-type excited-state method is straightforward. Employing the algebraic-diagrammatic construction (ADC) scheme of up to third order as well as time-dependent density-functional theory (TD-DFT), we demonstrate and evaluate the approach. For this purpose, we assembled a set of experimental benchmark data for solvatochromism in molecules (xBDSM) containing 44 gas-phase to solvent shifts for 17 molecules. These data are compared to solvent shifts calculated at the ADC(1), ADC(2), ADC(3/2), and TD-DFT/LRC-ωPBE levels of theory in combination with state-specific as well as linear-response type PCM-based correction schemes. Some unexpected trends and differences between TD-DFT, the levels of ADC, and variants of the PCM are observed and discussed. The most accurate combinations reproduce experimental solvent shifts resulting from the bulk electrostatic interaction with maximum errors in the order of 50 meV and a mean absolute deviation of 20−30 meV for the xBDSM set.

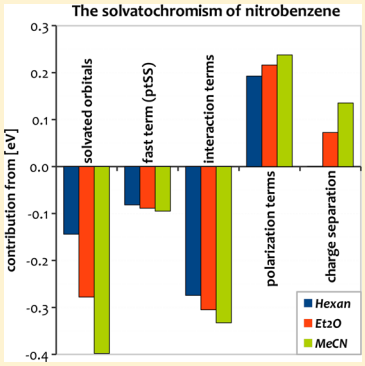

I. INTRODUCTION

Apart from atmospheric and interstellar chemistry, most photochemical problems occur in condensed phases, where the molecular environment may significantly affect the photophysical and photochemical processes. Therefore, any investigation of electronic excitation energies in a condensed-phase system should include at least an estimate of the influence of the environment on the transitions of the chromophore. The direct approach, which is to fully include the relevant environment explicitly in the quantum chemical calculation is not feasible due to the huge number of atoms that would be required to recover the bulk electrostatic interaction with the environment in combination with the steep exponential scaling of the computational effort for accurate quantum chemical methods with respect to system size. Hence, the approximate modeling of molecular environments in quantum-chemical problems in the condensed phase is a very active field of research.[1−8]

Condensed-phase problems may in general be subdivided into two groups: on the one hand, chromophores embedded in an essentially isotropic environment (e.g., solvent, nonpolar polymer matrix) and, on the other hand, chromophores surrounded by an anisotropic environment (e.g., protein, polar polymer matrix). For the latter, polarizable continuum models (PCMs) are only of limited applicability, because specific interactions between the chromophore and the anisotropic environment are usually of key relevance. Hence, an atomistic modeling of the environment is indispensable. This can be achieved using, e.g., QM/MM,[2,3,6,7] fragment-based,[4,5] or symmetry-adapted perturbation-theoretical (SAPT) approaches.[8] In exchange for the ability to describe an explicit environment, these models are usually quite demanding with respect to both time required for setup and evaluation of numerous parameters (force field, embedding scheme, partitioning, cut-offs, etc.). Moreover, the computational demand for such explicit approaches is inherently many times higher than for a single quantum-chemical calculation *in vacuo*. This is due to the need for sampling, which means an averaging over tens to hundreds of explicit configurations to capture the thermal equilibration of the environment.

Special Issue: Jacopo Tomasi Festschrift

Received: November 7, 2014
Revised: January 14, 2015
Published: January 28, 2015

DOI: 10.1021/jp511163y
J. Phys. Chem. A 2015, 119, 5446−5464

For chromophores in isotropic liquid solution, polarizable continuum models[1] (PCMs) offer an efficient way to incorporate bulk electrostatic effects, which are usually the most important solvation effects for small molecules. Once the construction of a molecular cavity for the solute is specified, these are essentially "black box" computational models. In many cases, the QM/PCM approach can be used to estimate the influence of the environment in one single calculation as it circumvents the problem of sampling. The equilibration of the solvent is already included in the dielectric constant, ϵ. To the extent that the temperature and frequency dependence of ϵ have been characterized experimentally, variation of ϵ allows for a straightforward investigation of these dependencies.

The remainder of this work is organized as follows. In section II, we introduce the concept of PCMs and the extension to vertical excitations, discuss the accuracy of the model, and motivate an evaluation based on a comparison to experimental data. In section III, we introduce the formalism for quantum-chemical calculations of vertical excitation energies within a PCM framework. In section IV, we describe the experimental results that are used to construct a benchmark data set. Finally, in section V results of the ADC and TD-DFT calculations are discussed and compared to our novel xBDSM set.

II. GENERAL CONSIDERATIONS

A. Polarizable Continuum Model. The central idea underlying PCMs is to include the electrostatic interaction of a molecule with an isotropic environment (usually a solvent) using the macroscopic dielectric polarizability of the environment. For this purpose, one needs to partition the system into molecule (solute) and environment (solvent), which gives rise to the molecular cavity. The construction of the cavity is nontrivial and often critical for the accuracy of the PCM,[9] but it is not an issue that we will explore in this work.

Employing a boundary-element procedure that solves for the surface charge arising from the discontinuous change in the dielectric constant for a classical charge distribution within the cavity, the solution of Poisson's equation can be circumvented.[10] Volume polarization, arising from the tail of the quantum-mechanical density, is included approximately by modifying the apparent surface charge (ASC). Two procedures for this were developed independently and are now widely used in quantum chemistry: the "integral equation formulation" (IEF-PCM) of Cancés, Mennucci, and Tomasi,[11,12] and the "surface and simulation of volume polarization for electrostatics" [SS(V)PE] approach developed by Chipman.[13,14] Although these methods are formally equivalent,[15,16] some differences arise when the integral equations are discretized for practical calculations.[10,17] We use the "asymmetric" version of SS(V)PE, which is recommended in ref 17, as implemented in the Q-Chem program[18] via an intrinsically smooth discretization procedure.[19]

For an investigation of vertical excitations in a PCM framework, the frequency dependence of the dielectric susceptibility must be considered, at least approximately. The response of the PCM environment depends on the time scale of the molecular process under investigation, because the dielectric polarization includes both slow (orientational and vibrational) components and fast (electronic) contributions. Because the atomistic environment is replaced by a continuum, and because the underlying quantum-chemical model is a time-independent one, the consequences of time-dependent polarization have to be introduced explicitly. The formalism is summarized in section IIIB. For a complete and detailed derivation starting from basic electrostatics, see ref 20.

B. Considerations for Excited States. The accuracy of the PCM treatment of solvation effects is limited mainly by a number of factors. First, only bulk electrostatic interactions are included at this level, and the accuracy will suffer when "specific" solvent effects are important. A prototypical example is a chromophore with a phenolate group, for which strong ionic hydrogen bonding directly affects the aromatic core. This effect becomes notable already if there are slightly acidic protons, e.g., in 3- and 4-nitroaniline and a slightly Lewis-basic solvent such as diethyl ether (Et_2O) or acetonitrile (MeCN). Such cases can usually be handled by the introduction of few explicit solvent molecules to the quantum system. The impact of hydrogen bonding as well as the introduction of explicit solvent molecules on the accuracy of the PCM have been examined in section VG.

Second, excitonic coupling between multiple choromophores may alter excitation energies. It has been inferred that this effect can be described within the PCM formalism by the so-called linear-response approach,[21] which is obtained when time-dependent perturbation theory is applied to the QM/PCM system.[22] Ultimately, the excitonic coupling of the excited states is described by the interaction of the induced polarizations of the respective transition densities. However, this requires a modification of the secular matrix of the CI problem prior to diagonalization, which goes beyond an exclusively density-based *a posteriori* correction. An implementation of this approach in combination with the COSMO solvent model[23] and the ADC(2) quantum chemistry approach has recently been reported.[21]

A third problem that has attracted much less attention in the literature is the limitation of PCMs due to the approximate nature of the underlying quantum chemical model. This becomes particularly relevant when approximate linear response methods such as TD-DFT or ADC(1) are used, especially in the context of highly correlated or charge-transfer (CT) excited states. Although problems with CT excitation energies in TD-DFT[24,25] have to a large extent been resolved by the introduction of range-separated functionals,[26−29] it is not clear how well this correction performs for the excited-state densities that will afford the solvation correction.[30]

Another issue of post-Hartree−Fock methods within the PCM framework is the appropriate choice of reference state. For ADC(n) calculations, one usually employs the corresponding Møller−Plesset (MPn) ground state as a reference, which leads to several distinct ways how solvation effects might be included:[31−33]

(1) Use solvated Hartree−Fock (HF) orbitals for the MP2 calculation, in the so-called PerTurbation-Energy (PTE) scheme.
(2) Obtain the final solvation energy from an additional PCM calculation with the gas-phase MP2 density (PerTurbation-Density or PTD scheme).
(3) Iterate the PTD scheme until the MP2 density and solvent field are self-consistent (PerTurbation-Energy-and-Density or PTED scheme).

The schemes described above are sketched in Figure 1. As pointed out by Àngyàn,[34] only the PTE scheme yields an energy that is formally consistent with MP2 theory, whereas the PTED scheme involves higher-order terms. Furthermore, the PTED scheme is computationally more involved, in particular

DOI: 10.1021/jp511163y
J. Phys. Chem. A 2015, 119, 5446−5464

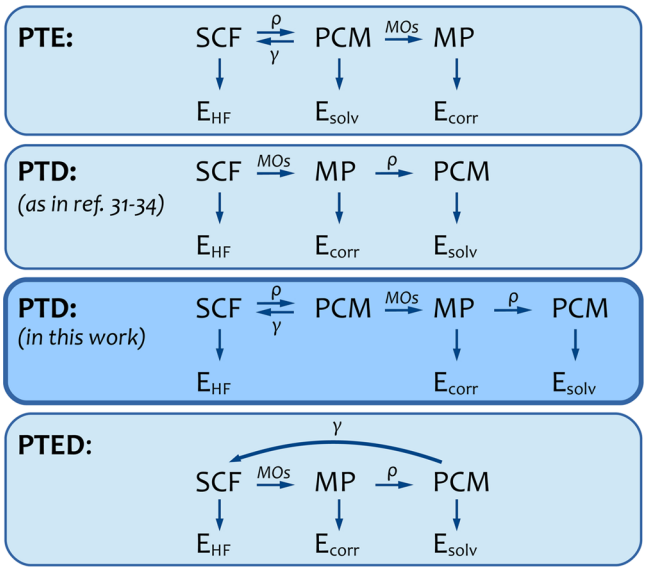

Figure 1. Flowchart of the different approaches to include electron correlation in a PCM framework. Here, ρ refers to the charge density and γ to the surface charge. The down-pointing arrows indicate at which point in the procedure HF, solvation, and correlation energies are computed. The simplest PTE scheme employs the polarized HF MOs for the subsequent MP calculation, whereas the PTD and PTED schemes involve a PCM calculation for the correlated density. For the original PTD scheme, the solvation energy is computed once for the gas-phase MP density, thereby neglecting the self-induced polarization of the solute via the solvent. To include this self-induced polarization, our implementation of the PTD scheme employs the MP density computed for the self-consistently polarized HF MOs. Within the most expensive PTED scheme, the MP density and the solvent field are iterated to self-consistency.

for ADC(3), for which an MP3 ground-state density would have to be calculated multiple times. As such, we only examine results obtained with the PTE as well as a modification of the PTD scheme. (An implementation of the PTED scheme in combination with ADC(2) is described in ref 21). To the best of our knowledge, there exists neither a systematic investigation of the accuracy of predicted solvent shifts with respect to the level of electronic structure theory nor with respect to the choice of the ground-state reference. The present work reports such tests, for a variety of ADC-based methods, along with TD-DFT.

A fifth issue, which is beyond the scope of this work is due to the influence of the solvent onto the vibrational transitions in the chromophore. Because the influence of solvation will affect the Franck−Condon factors, which determine the intensity of the contributions building the optical spectrum, it can shift the maximum of the experimentally determined absorption peak. Unfortunately, this effect cannot be accounted for with the presented methodology. Already in the gas phase, the calculation of vibrationally resolved spectra is challenging.[35,36] To circumvent the explicit calculation of vibronic couplings, we focus on solvent-induced shifts, which essentially neglects all solvent-induced differences of the vibronic couplings in the optical spectra.

C. Evaluation of Solvent Models by Comparison to Experimental Solvatochromic Shifts. In comparing PCM solvent shifts to experimental ones, it is important to understand the various effects that contribute to the shift. In quantum chemical terms, these include

(1) differences between the ground-state equilibrium geometry in the gas versus solution phase,
(2) "zeroth-order" contributions arising from the polarization of the ground-state wave function by the solvent,
(3) "first-order" corrections arising from the fast, electronic component of the solvent's dielectric susceptibility, and
(4) nonelectrostatic interactions that change upon electronic excitation.

The size of these contributions strongly depends on the particular molecule. For example, in molecules exhibiting negative solvatochromism (blue-shift upon increasing solvent polarity), geometrical contributions actually make up the blue part of the shift, whereas first-order contributions are always negative (red shift). To keep geometrical contributions small, and thereby focus on the electrostatic contributions, we have exclusively selected molecules exhibiting solvatochromic red shifts for our benchmark set, although the influence of geometry is taken into account in our calculations. Nonelectrostatic contributions arise primarily from the energetic cost of cavity formation ("cavitation energy"), which may be expected to cancel for vertical excitation, and for changes in dispersion and Pauli repulsion energies upon electronic excitation, which are usually neglected.

Another problem in the evaluation of calculated solvent shifts becomes evident when we analyze the various contributions of nonpolar to polar (e.g., cyclohexane to acetonitrile) solvent shifts. We find that these arise exclusively due to differences in the zeroth-order contributions, whereas the first-order contributions cancel quantitatively. This is traceable to the very small variation in the optical dielectric constant ($=n^2$, where n is the index of refraction) across common solvents, whereas the static dielectric constant varies significantly (Table 1).

Table 1. Dielectric Constants Used in the Calculations

solvent	static dielectric, ε	optical dielectric, n^2
hexane	1.89	1.88
cyclohexane (cyHex)	2.03	2.02
dioxane (Diox)	2.21	2.02
diethyl ether (Et_2O)	4.32	1.83
acetonitrile (MeCN)	36.7	1.81
dimethyl sulfoxide (DMSO)	46.7	2.07
water (H_2O)	80.4	1.78

The small variations in n^2 suggest that a meaningful evaluation of PCM corrections must consider gas-phase to solution shifts, rather than solvent-to-solvent shifts. However, gas-phase data of large, i.e., nonvolatile, molecules are scarce in the literature and place constraints upon the size and polarity of the molecules. Consequently, our benchmark set consists of small- to medium-sized organic compounds that can be evaporated under application of mild heat and/or low pressure. Moreover, each molecule needs to have a distinct absorption peak caused by a single transition that has no or little overlap with other transitions, because otherwise the analysis of the spectrum is significantly more complicated. These conditions are largely fulfilled for mono- and disubstituted nitroaromatics, for which experimental gas-phase and solvent excitation energies are available.[37−40] In addition, we have recorded gas-phase and solvent spectra for the prototypical aromatic compounds pyridine (Py), benzofuran (Bf), coumarin (Cm), and nitrobenzene (NB).

DOI: 10.1021/jp511163y
J. Phys. Chem. A 2015, 119, 5446−5464

III. FORMALISM AND IMPLEMENTATION

This section briefly describes our PCM formalism for vertical excitation energies; for a detailed derivation, see ref 20. The basic concept of the state-specific solvent correction was first introduced by Yomosa in 1974,[41] and many subsequent formulations of the state-specific nonequilibrium formalism have since appeared.[21,42−44] The "ptSS" formalism[20] presented below is closely related to the corrected linear-response (cLR) approach of Caricato et al.[43] For a description of the ADC method, see ref 45 or 46.

A. Ground-State Equilibrium PCM. The starting point for the calculation of excitation energies in solution is a converged HF or Kohn−Sham (KS) self-consistent field (SCF) calculation for a molecule in a cavity with the surface S subdivided into surface elements s. (In our implementation these are Lebedev grid points situated on atomic spheres.[19]) In this self-consistent reaction field (SCRF) calculation, the effect of the PCM is contained in the reaction-field potential operator, $\hat{R}(0)$:

$$[\hat{H}^{\mathrm{vac}} + \hat{R}(0)]|0\rangle = E_0|0\rangle \tag{1}$$

which is

$$\hat{R}(i) \equiv \hat{R}_i \equiv \int_S \frac{\gamma_i(s)}{|r-s|}\,\mathrm{d}s = \int_S \hat{V}(r,s)\,\gamma_i(s)\,\mathrm{d}s \tag{2}$$

For the sake of compactness, we introduced the operator $\hat{V}(r,s) = |r-s|^{-1}$, which formally corresponds to a measurement of the electrostatic potential (ESP) of the wave function on the surface s. The expression can be simplified even further by carrying out the implicit integration over r (eq 3), which yields the function $V_0(s)$ for the ESP of the wave function $|0\rangle$ at the position s. The integration of the product of this function with the surface charge $\gamma_i(s)$ over the cavity surface s yields the interaction energy of $|0\rangle$ with the polarization induced by $|i\rangle$.

$$\begin{aligned}\langle 0|\hat{R}_i|0\rangle &= \int_S \langle 0|\hat{V}(r,s)|0\rangle\,\gamma_i(s)\,\mathrm{d}s \\ &\equiv \int_S V_0(s)\,\gamma_i(s)\,\mathrm{d}s \\ &\equiv E_{0-i}\end{aligned} \tag{3}$$

If solute and solvent are in equilibrium (e.g., in the case of a ground or long-lived excited state), the molecule interactions with its self-induced polarization and $|0\rangle$ and $|i\rangle$ in eq 3 are identical. In practice, $\gamma(s)$ in $\hat{R}$ is represented by a set of Gaussian-blurred point charges at the positions of the surface elements s, which are the numerical realization of the so-called apparent surface charge (ASC) (Figure 2). In contrast to fixed point charges of, e.g., a QM/MM calculation, the ASC in an SCRF calculation does itself depend on the molecular charge distribution and is thus updated in every iteration. To obtain the ASC $\gamma(s)$ for a given wave function, one may formulate a surface-charge operator

$$\hat{Q} \equiv \int_S \hat{V}(r,s')\,A_\varepsilon^{-1}(s,s')\,\mathrm{d}s' \tag{4}$$

which contains the so-called PCM kernel A_ε^{-1}. This kernel depends on the cavity geometry and the dielectric constant of the medium and is what discriminates between various flavors of PCM. Formally, it is used to solve the Poisson problem, or in other words to convert the molecular ESP into an ASC $\gamma(s)$. Due to the self-interaction of the ASC, the kernel for the charge on a fraction s of the surface depends upon the molecular ESP as well as the ESP of the charge on the remaining surface $\gamma(s')$. Applied to a wave function $|i\rangle$, $\hat{Q}$ yields the ASC $\gamma_i(s)$ resembling the polarization of the dielectric continuum with the dielectric constant ϵ.

$$\gamma_i(s) = \langle i|\hat{Q}|i\rangle = \int_S V_i(s')\,A_\varepsilon^{-1}(s,s')\,\mathrm{d}s' \tag{5}$$

It is important to stress that during the SCRF calculation the solute wave function and its reaction field are iterated to self-consistency. As a result, the polarized MOs building the reference-state wave function contain the interaction with the ASC in the form of orbital energies. Any post-HF procedure therefore includes the interaction with the equilibrated ground-state solvent field, just as the mean-field electron−electron interaction and/or any interaction with any classical point charges would be included, in a QM/MM calculation, for example. This will become relevant for the discussion of nonequilibrium situations in the next section.

B. Vertical Excitations in the PCM Framework. Vertical excitation energies can be obtained via a CI-like procedure from the solvated ground-state reference wave function. To obey the Franck−Condon principle, only the fast (electronic) components of the polarization should be relaxed, whereas the slow (nuclear) component has to be kept frozen at its ground-state equilibrium. This is the so-called nonequilibrium limit for a very fast process in a PCM framework. To take this into account, the reaction-field is separated into fast (electronic) and slow (nuclear) components, starting with the operators. In the definitions of surface-charge and reaction-field operators (eqs 2 and 4) the solvent is is fully relaxed, which corresponds to the equilibrium case for the ground state. This means that the reaction field includes both fast (electronic) and slow (nuclear) contributions, which corresponds to ϵ as the (static) dielectric constant. In nonequilibrium situations, one needs to treat the fast component of the polarization separately. This can be achieved by replacing ϵ in A^{-1} (eq 4) with the optical dielectric constant n^2 by introducing the effect of the slow component (eq 19).[20] The slow component of ϵ is replaced by $\epsilon - n^2$. Accordingly, one may split the reaction-field and surface charge operators into fast and slow components:

$$\hat{Q}^{\mathrm{s+f}} = \hat{Q}^{\mathrm{s}} + \hat{Q}^{\mathrm{f}} \tag{6a}$$

$$\hat{R}^{\mathrm{s+f}} = \hat{R}^{\mathrm{s}} + \hat{R}^{\mathrm{f}} \tag{6b}$$

A Hamiltonian for an out-of-equilibrium excited state $|i\rangle$ that is in accordance with the Franck−Condon principle can now be constructed:

$$E_i^{\mathrm{NEq}} = \langle i|\hat{H}^{\mathrm{vac}} + \hat{R}_0^{\mathrm{s}} + \hat{R}_i^{\mathrm{f}}|i\rangle \tag{7}$$

This Hamiltonian is, however, not practical, as it is different for each excited state (i.e., state specific) and therefore sacrifices orthogonality between states as well as certain sum rules for oscillator strengths.[47] A solution is suggestive if the proportions of the underlying problem are considered. First, the potential introduced through the fast polarization component is small with respect to the potential of the solute nuclei, and second the change in electron density upon excitation is small with respect to the whole solute density. Hence, the response of the solvent to excitation of the solute can be treated in perturbative fashion:

$$E_i^{\mathrm{NEq}} = \langle i|\hat{H}^{\mathrm{vac}} + \hat{R}_0^{\mathrm{s+f}} + \lambda(\hat{R}_i^{\mathrm{f}} - \hat{R}_0^{\mathrm{f}})|i\rangle \tag{8}$$

DOI: 10.1021/jp511163y
J. Phys. Chem. A 2015, 119, 5446−5464

Taking into account that the actual zeroth-order Hamiltonian contains the frozen reaction field of the ground state,

$$E_i^{(0)} = \langle i^{(0)}|\hat{H}^{\mathrm{vac}} + \hat{R}_0^{\mathrm{s+f}}|i^{(0)}\rangle \tag{9}$$

one obtains a first-order correction

$$E_i^{(1)} = \langle i^{(0)}|\hat{R}_i^{\mathrm{f}} - \hat{R}_0^{\mathrm{f}}|i^{(0)}\rangle \tag{10}$$

Eventually, the problematic state-specific (SS) Hamiltonian (eq 7) is converted into a perturbative correction, which can be computed *a posteriori* using the zeroth-order wave function $|i^{(0)}\rangle$. The latter is obtained from a CI-type calculation based on polarized ground-state MOs. To emphasize the perturbative nature of the approach, it will be denoted as perturbation-theoretical state-specific (ptSS)-PCM.

For the evaluation of eq 10 one needs the fast polarization charges of the ground state. To compute these, the ground-state reaction field can be separated on the basis of the respective dielectric constants for slow (ϵ) and fast (n^2) polarization:[22]

$$\gamma^{\mathrm{s}} = \left(\frac{\epsilon - n^2}{\epsilon - 1}\right)\gamma^{\mathrm{total}} = \gamma - \gamma^{f} \tag{11a}$$

$$\gamma^{\mathrm{f}} = \left(\frac{n^2 - 1}{\epsilon - 1}\right)\gamma^{\mathrm{total}} \tag{11b}$$

When the charges are separated in this way, one must mind the self-interaction between fast and slow ground-state surface charges according to

$$E_{\mathrm{s-f}} = \int_S \gamma_0^{\mathrm{f}}(s)\, V_{\gamma_0^{\mathrm{s}}}(s)\, \mathrm{d}s \tag{12}$$

where $V_{\gamma_0^{\mathrm{s}}}(s)$ is the ESP of the slow, ground-state polarization charges at the position s. In analogy to the molecular ESP, it can be obtained by integrating the slow component of ASC resembling the ground-state polarization

$$V_{\gamma_0^{\mathrm{s}}}(s) = \int_S \frac{\gamma_0^{\mathrm{s}}(s')}{|s' - s|}\, \mathrm{d}s' \tag{13}$$

If the fast ASC obtained for the ground state is now replaced by the fast ASC of an excited state $\gamma_i^{\mathrm{f}}(s)$, this interaction changes. To account for this, a charge-separation correction is introduced:

$$E_{\mathrm{cs}} = \int_S (\gamma_i^{\mathrm{f}}(s) - \gamma_0^{\mathrm{f}}(s))\, V_{\gamma_0^{\mathrm{s}}}(s)\, \mathrm{d}s \tag{14}$$

C. Free Energy. Because the dielectric constant implicitly includes solvent averaging, the electrostatic energies in PCM theory are *free* energies, whereas up to this point we have introduced expressions for interaction energies only. To obtain free energies, one must account for the work associated with polarizing the continuum, which amounts to half of the electrostatic interaction energy.[48,49] Thus, the free energy of the equilibrated system in its ground state is

$$G^{\mathrm{solv}} = \langle 0|\hat{H}^{\mathrm{vac}}(0) + \frac{1}{2}\hat{R}_0|0\rangle \tag{15}$$

For an excited state in the nonequilibrium limit, the derivation of the polarization work is more involved. It includes the charge-separation correction (eq 14) as well as further terms for the polarization work involving the fast charges in both ground and excited states. For a detailed derivation and discussion of these terms, see ref 20. Finally, the first-order ptSS correction to the $|0\rangle \rightarrow |i\rangle$ excitation energy is given as

$$\begin{aligned} G_i^{\mathrm{ptSS}} = {} & \langle i^{(0)}|\hat{R}_i^{\mathrm{f}}|i^{(0)}\rangle - \langle i^{(0)}|\hat{R}_0^{\mathrm{f}}|i^{(0)}\rangle \\ & - \frac{1}{2}(\langle i^{(0)}|\hat{R}_i^{\mathrm{f}}|i^{(0)}\rangle - \langle 0|\hat{R}_0^{\mathrm{f}}|0\rangle) \\ & + \frac{1}{2}\int_S (\gamma_i^{\mathrm{f}}(s) - \gamma_0^{\mathrm{f}}(s))\, V_{\gamma_0^{\mathrm{s}}}(s)\, \mathrm{d}s \end{aligned} \tag{16}$$

Here, the interaction terms are collected in the first line whereas the remaining terms constitute the polarization work.

D. Electron Correlation Corrections: The PTD Scheme. For calculations employing the PTE scheme, γ^{total} in eq 11 refers to the ASC obtained for the ground-state HF or KS density. In post-HF methods, this introduces a systematic error in solvent shifts if the ground-state ESP is not well described at the HF level of theory because the ground-state reaction field enters the zeroth-order excitation energies via the polarized MOs. This is indeed the case for nitroaromatics, for which the total MP2 dipole moment is only 80% of the HF dipole moment. Account for this effect, we introduce the following correction to the zeroth-order excitation energy:

$$\begin{aligned} E_{\mathrm{PTD}}^{(0)} = {} & (\langle i^{(0)}|\hat{R}_{0^{\mathrm{MP}}}|i^{(0)}\rangle - \langle 0^{\mathrm{MP}}|\hat{R}_{0^{\mathrm{MP}}}|0^{\mathrm{MP}}\rangle) \\ & - (\langle i^{(0)}|\hat{R}_{0^{\mathrm{HF}}}|i^{(0)}\rangle - \langle 0^{\mathrm{MP}}|\hat{R}_{0^{\mathrm{HF}}}|0^{\mathrm{MP}}\rangle) \\ = {} & \langle i^{(0)}|\hat{R}_{0^{\mathrm{MP}}} - \hat{R}_{0^{\mathrm{HF}}}|i^{(0)}\rangle - \langle 0^{\mathrm{MP}}|\hat{R}_{0^{\mathrm{MP}}} + \hat{R}_{0^{\mathrm{HF}}}|0^{\mathrm{MP}}\rangle \end{aligned} \tag{17}$$

Adding this correction, the zeroth-order interaction of the difference density of the excited state with the polarization of the HF ground state ($|0^{\mathrm{HF}}\rangle$, lower term) is replaced by the interaction of the difference density of the excited state with the polarization of the Møller−Plesset (MP) ground state ($|0^{\mathrm{MP}}\rangle$, upper term). Within our implementation of the PTD scheme, the employed HF reaction field is obtained self-consistently, but the MP reaction field is calculated from the MP density computed with polarized HF orbitals (Figure 1). Because the latter are overly polarized in the case of nitroaromatics, the MP reaction will also contain this error and the correction will be incomplete and is presumably smaller than the error introduced by the HF reaction field. However, as compared to the iterative PTED scheme, this PTD correction has the advantage that it can be calculated *a posteriori*, which is in accordance with all other corrections terms introduced above.

The first-order terms also differ between the PTE and PTD schemes, because the response of the polarization has to be calculated in the presence of the slow component of the ground-state reaction field (eq 19). Consequently, γ^{total} in eq 11 refers to the ASCs obtained for the MP ground-state density. Accordingly, for the PTD scheme all other terms that explicitly depend upon the ASC of the ground state (eqs 2, 10, 14, 16, and 19) use MP densities. To distinguish between the PTE and PTD approaches for the ADC(2) and ADC(3/2), the abbreviation ptSS-PCM(PTE) and ptSS-PCM(PTD) will be used.

E. Perturbative Linear-Response-Type Corrections. In addition to the state-specific corrections described above, we have implemented *perturbative* linear-response (LR) correction terms. These are obtained by keeping only the diagonal elements of the original LR *ansatz* described in ref 50 for TD-HF and in ref 21 for ADC. As compared to the latter formulation, however, we use a different partition of the

DOI: 10.1021/jp511163y
J. Phys. Chem. A 2015, 119, 5446−5464

Hamiltonian, to obtain the same formalism for the zeroth-order terms of the LR and SS approaches, which are in fact the same.[51] Consequently, we identify the first two terms in the diagonal elements of the free energy matrix (eq 17 in ref 21) as our zeroth-order energy (eq 9 in this work). For our perturbative LR-type corrections (ptLR-PCM), we add the energy of the third term in eq 17 of ref 21 to our zeroth-order result. Because we neglect all off-diagonal elements for our perturbative corrections, this term corresponds to the interaction of the transition density with the dielectric medium:

$$E_i^{\mathrm{ptLR}} = \int_S \langle i^{(0)}|\hat{V}(r,s)|0\rangle \gamma_{\mathrm{lr}}(s)\, \mathrm{d}s \tag{18a}$$

$$\gamma_{\mathrm{lr}}(s) = \int_S \langle i^{(0)}|\hat{V}(r,s')|0\rangle A_{n^2}^{-1}(s,s')\, \mathrm{d}s' \tag{18b}$$

Although this ptLR correction is itself independent of the PTE and PTD schemes, one can combine these corrections with the zeroth-order terms for both, affording what we designate as the ptLR-PCM(PTE) and ptLR-PCM(PTD) schemes.

In the case of an isolated bright state, the ptLR-PCM approach yields results that are reasonably close to the full, self-consistent LR approach, as demonstrated below. The advantage is that the ptLR corrections can be calculated *a posteriori*, without a manipulation of the secular matrix of the CI problem. However, this approximation can break down if there are additional bright excited states in close proximity, as, e.g., in the case of coumarin.

F. Excited-State Densities. Excited-state densities are required to compute the ESP for $|i^{(0)}\rangle$. Formally, these can be obtained from the excited-state wave function, which corresponds to an unrelaxed density, or by computing the energy-derivative with respect to an electric field, yielding a relaxed density.[52] For linear-response methods, only the relaxed density corresponds to an observable quantity, because the response vectors themselves have no physical meaning. This is reflected in the results of the TD-DFT calculations, where unrelaxed densities yield first-order corrections that are too large. Consequently, the solvent shifts are systematically overestimated in all cases using unrelaxed TD-DFT densities, as shown in section VF4). A recent study of 4-nitroaniline also confirms that only relaxed TD-DFT densities are in good agreement with multireference CI calculations.[53] Hence, we use relaxed densities for the TD-DFT calculations.

For ADC calculations, we obtain the densities via the intermediate-state-representation (ISR) formalism consistent with the given order in perturbation theory.[46] ADC is not a linear response method, and these densities are not "relaxed" in the aforementioned sense (i.e., they do not include explicitly calculated orbital relaxations). Nevertheless, they do contain significant orbital relaxation effects, as demonstrated recently at second order,[54,55] and are inexpensive to compute. For this purpose, the converged ADC excited-state vectors are combined with the intermediate-state basis of the appropriate order, yielding an excited-state wave function. Eventually, the excited-state densities used for the PCM calculations are consistent to first order for ADC(1) and to second order for ADC(2). For ADC(3), an efficient implementation of the ISR of corresponding order is not yet available, so the ISR of second order is used in combination with the ADC(3)-state vectors. This is the definition of the mixed ADC(3/2) approach.

G. Technical Details of the Implementation. After convergence of the SCRF calculation (eq 1), the ground-state reaction field is split into fast and slow components according to eq 11. Using the polarized MOs, a CI-type calculation (ADC or TD-DFT in this work) is carried out, which affords the correlated ground-state density as well as the zeroth-order excited-state vectors and excitation energies (eq 9). To obtain the first-order corrections, the terms in eq 16 have to be calculated. This requires construction of $\hat{R}_i^{\mathrm{f}}$, which in turn requires the ASC resembling the fast component of the polarization for the excited state $|i^{(0)}\rangle$. This is obtained by using a modified version of the surface-charge operator eq 4, in which ϵ is replaced by n^2 and the ESP of the slow ground-state polarization charges (eq 13) is added to the molecular ESP, $V_{i(0)}(s')$:[22,44]

$$\gamma_i^{\mathrm{f}}(s) = \int_S (V_{\gamma_0^{\mathrm{s}}}(s') + V_{i^{(0)}}(s'))A_{n^2}^{-1}(s,s')\, \mathrm{d}s' \tag{19}$$

With the surface charges, $\hat{R}_i^{\mathrm{f}}$ can be constructed and all first-order interaction and polarization terms can be evaluated. The numerical procedure is sketched for the example nitrobenzene in Figure 2.

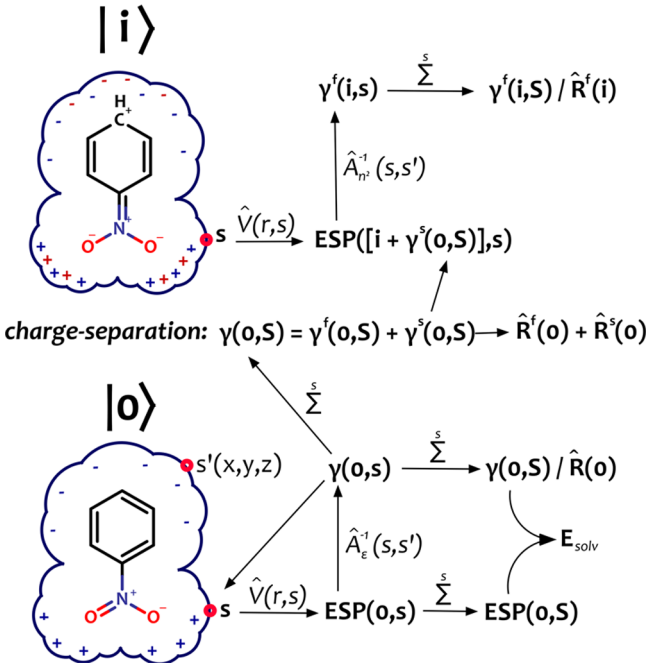

Figure 2. Flowchart of the numerical procedure of a nonequilibrium state-specific PCM calculation for a vertical excitation from the ground state $|0\rangle$ to the excited state $|i\rangle$. The integration over s is replaced by a finite sum over the surface elements. The ground-state polarization of the surface charges is depicted in blue, the response of the fast component to the increased dipole moment of the excited state in red. The notation is very similar to that in the article, except for the electrostatic potential for which we use the notation ESP(state,s) instead of $V_0(s)$.

To obtain corrected vertical excitation energies for the PTE scheme, the first-order corrections are just added to the zeroth-order excitation energies. However, for calculation of the fast polarization and first-order terms within the PTD scheme, the ground-state polarization of the correlated ground state is required. To obtain it, eq 4 is solved for correlated MP density, which in contrast to the original PTD scheme is calculated using the polarized HF MOs. The zeroth-order PTD corrections (eq 17) contain additional terms. These are the

DOI: 10.1021/jp511163y
J. Phys. Chem. A 2015, 119, 5446−5464

interaction of the excited-state densities with the ground-state polarization of both the MP and HF ground states, as well as the interaction of the MP density with the HF reaction field. All these terms are calculated after the CI calculation-type using the respective reaction fields.

IV. METHODOLOGY

A. Technical Details. Gas-phase as well as solvent-relaxed geometries were obtained at the B2-PLYP/def2-TZVP level of theory,[56,57] in combination with Grimme's D3 dispersion correction[58] and the COSMO solvation model[59] as implemented in Orca 3.0.1.[60] This level of theory has previously been found to provide good agreement with experiment for a prototypical nitrobenzene, whereas MP2-, CC2-, and CCSD-optimized geometries deviated significantly.[61] In the case of the amino-methoxy disubstituted nitroaromatics, we find that the dispersion correction systematically improves the predicted solvent shifts, for all QM/PCM combinations considered here. Optimized geometries are available in the Supporting Information.

A comparison to shifts computed with ADC(2)/ptSS-PCM(PTE) and ptLR-PCM(PTE) for gas-phase and solvent-relaxed geometries obtained at the SCS-MP2/cc-pVTZ level of theory using the COSMO solvation model and the PTE approach can be found in the Supporting Information. The results for the two sets of geometries are very similar (MAD 0.022 eV).

All CI-type calculations (ADC and TD-DFT) were carried out using a locally modified version of Q-Chem 4.2,[18] and employ the cc-pVDZ basis set.[62] For the TD-DFT calculations, the LRC-ωPBE functional has been employed, which has been found to be very accurate for calculation of vertical excitation energies if the range-separation parameter is tuned systematically.[63,64] For this purpose, ω is chosen such that HOMO and LUMO energy equal the ionization potential and electron affinity, respectively.[65] This procedure leads to ω values of 0.27−0.32 a.u. for the molecules in the xBDSM set, which is close to the standard value of 0.3 a.u. The cavity for the PCM calculations in Q-Chem is obtained using a smooth Lebedev-grid based construction algorithm,[19] with Bondi's atomic van der Waals radii[66,67] scaled by a factor of 1.2.

B. Experimental Data. Experimental data for the *meta*- and *para*-substituted nitroaromatic compounds were obtained from ref 38. Data for the methoxy-nitroanilines was taken from ref 39. Data for 4-nitrophenolate and 4-(4-nitrophenyl)-phenolate were obtained from ref 68.

For nitrobenzene, benzofuran, coumarin, pyridine, and 4-nitroaniline UV/vis spectra were recorded in the gas phase and in Hex and MeCN, and for 4-nitroaniline also in dioxane. The UV/vis-transmission spectra were recorded using a PerkinElmer-Lambda 750 spectrometer operated at a resolution of 0.5 nm. A 10 mm quartz glass (Suprasil-Hellma) was used. The average concentration of the compounds (purities grade >99%) in solution has been adjusted between 0.1 and 0.01 mM. To obtain transmission spectra in the gas phase, a small quantity of the compound was filled into the sealable cuvette or, in the case of pyridine, a gaseous injection was taken from the original bottle. In the case of coumarin, mild heat was applied to achieve a sufficient concentration in the gas phase. The peak-finding algorithm implemented in the PerkinElmer Spectra Suite software was used to determine maxima and solvent shifts. In the case of coumarin and benzofuran, whose absorption spectra exhibit vibrational structure, the differences were determined between the most distinct features of the respective peaks. This is sufficient because we are not interested in absolute but in relative energies (solvent shifts) between the electronic transitions. Experimental reference data are available in the Supporting Information.

V. RESULTS AND DISCUSSION

A. Characterization of the Excited States. The experimental data for the monosubstituted nitroaromatics always refer to the first peak in the absorption spectrum. For all but two of the nitroaromatic molecules, our calculations reveal that the first bright state is closely related to the $2A_1$ $\pi\pi^*$ excited state of nitrobenzene (NB), which is almost exclusively characterized by the HOMO−1 to LUMO transition. This excited state has significant CT character in NB, with a dipole moment that increases from 4.3 D in the ground state to 10.0 (8.9) D in the excited state at the MP2/ADC(2) (ADC(3,2)) level of theory. Only in the *meta*-substituted isomers of the push−pull systems 3-nitroanisole (3-methoxy-NB) and 3-nitroaniline (3-amino-NB) is a different state responsible for the first peak. In these two cases, it is related to the $1B_1$ $\pi\pi^*$ state of NB, which is symmetry forbidden in the parent NB. In molecules with an electron-pushing substituent in the *meta* position, however, it has enough oscillator strength to appear in the spectrum. This state is characterized by the HOMO → LUMO transition, whereas the dipole moment is increased to 5.8 (6.3) D at the ADC(2) (ADC(3,2)) level of theory for NB. These states have been extensively characterized for NB.[61]

In pyridine, benzofuran, and coumarin we investigate the shifts of the lowest $\pi\pi^*$ excitation(s). In pyridine, the ground-state dipole moment of 2.0 D is slightly decreased in the first bright state (S_3, 1.8 D, HOMO → LUMO and HOMO−1 → LUMO+1 transition). In benzofuran, the ground-state dipole moment of 0.6 D is hardly affected in the first bright state (S_1, 0.7 D, HOMO−1 → LUMO and HOMO → LUMO+1 transition) and slightly increased in the second bright state (S_2, 3.3 D, HOMO → LUMO and HOMO−1 → LUMO+1). In coumarin, the ground-state dipole moment of 4.2 D is hardly affected in the first bright state (S_1, 4.7 D, HOMO → LUMO, HOMO−1 → LUMO) and slightly increased in second bright state (S_3, 5.9 D, HOMO−1 → LUMO, HOMO → LUMO+1). All values correspond to gas-phase ADC(2)/cc-pVDZ//B2-PLYP+D3/def2-TZVP calculations.

B. Composition of the xBDSM Set. From the data available in the literature for monosubsituted nitroaromatics, we have chosen cyclohexane (cyHex), diethyl ether (Et_2O), and acetonitrile (MeCN) as representative solvents. According to eq 11, only the fast electronic polarization is relevant for the ground-state polarization cyHex (γ^f = 99% of γ^{total}), whereas for Et_2O both fast and slow components contribute significantly (γ^f = 25% of γ^{total}), whereas for MeCN the slow nuclear component dominates (γ^s = 98% of γ^{total}).

For the analysis of the results, the experimental data points are divided into three subgroups depending on molecule/solvent interactions and character of the excited states.

1. Exclusively Electrostatic Cases. This largest subgroup consists of the data points for nitrobenzene (NB) and the *meta*- and *para*-isomers of nitrotoluene (methyl-NB), nitroanisole (methoxy-NB), and nitrochlorobenzene (chloro-NB) in cyHex, Et_2O, and MeCN, as well as for *meta*- and *para*-nitroaniline (amino-NB) and the methoxynitroanilines (NH_2-MeO-NB) in cyHex. For this selection, the gas-phase to solvent shifts are for isolated bright transitions. Hence, the solvatochromic shift is

DOI: 10.1021/jp511163y
J. Phys. Chem. A 2015, 119, 5446−5464

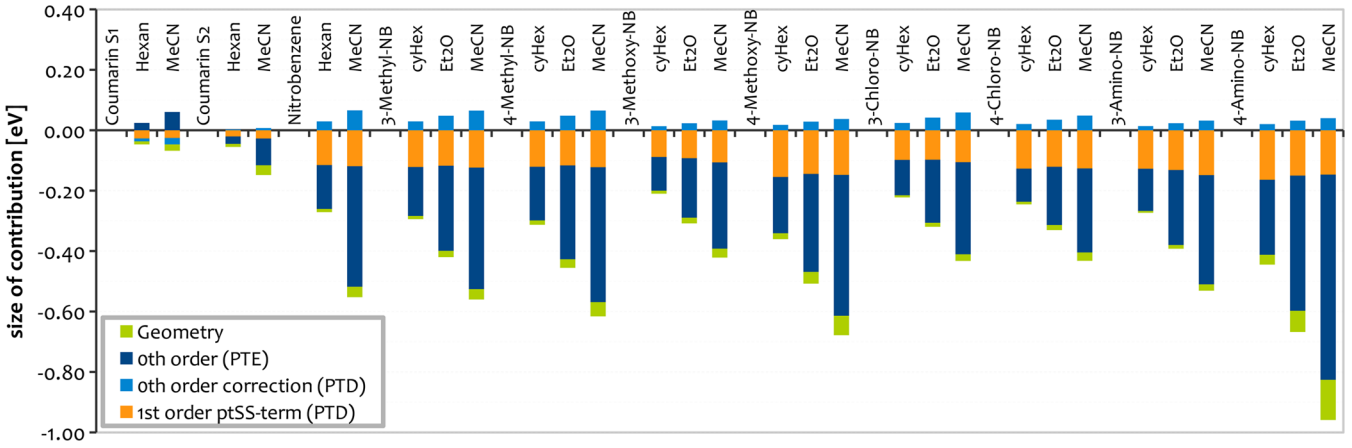

Figure 3. Breakdown of the calculated solvent shifts into geometrical, zeroth-order, and first-order contributions for selected examples at the ADC(2)/ptSS-PCM level of theory. In each case, the identity of the chromophore (coumarin S_1, coumarin S_2, nitrobenzene, etc.) is followed by a series of bar graphs representing different solvents.

almost exclusively due to the bulk electrostatic interaction, which should be accurately described by a proper PCM formalism.

On the basis of these examples, the accuracy of the first-order treatment of the fast response of the polarization is evaluated and the composition of the solvent shifts with respect to geometric, zeroth-order, and first-order contributions is analyzed. Moreover, the performance of the ptSS and ptLR approaches with respect to the level of electronic structure theory is examined and studied to determine how the treatment of correlation effects in the solvent model (PTE vs PTD) affects the results.

2. Cases Involving Hydrogen Bonding. These cases are also examples dominated by electrostatic effects, but they also involve hydrogen bonding with solvent molecules. The data points in this set comprise 4-nitroaniline in Et_2O, MeCN, dioxane (Diox), and dimethyl sulfoxide (DMSO), as well as 4-nitrophenolate (4-NP) and 4-(4′-nitrophenyl)phenolate (44-NPP) in water. On the basis of these examples, the impact of hydrogen bonding on the accuracy and is quantified and, furthermore, it is demonstrated how well this can be corrected-for by introduction of few explicit solvent molecules.

3. Nonelectrostatic Cases. This set includes molecules that exhibit hardly any experimental shift at all and have multiple bright excited states close in energy. These are pyridine, benzofuran, and coumarin in hexane and MeCN. This subset demonstrates how the ptLR correction behaves in difficult situations.

C. Composition of Calculated Shifts. In this section, the composition of the solvent shifts is examined using ADC(2)/ptSS-PCM(PTD) as a representative level of theory. An inspection of Figure 3 reveals that geometrical contributions to the shifts are small compared to the sum of zeroth- and first-order contributions. Although for clarity only a limited number of examples is shown in Figure 3, this applies to all molecules in the benchmark set. Only for 4-nitroaniline (termed 4-Amino-NB, far right in Figure 3) is the geometric contribution larger than 0.1 eV, which can be traced back to a solvent-dependent variation of the NH_2 out-of-plane bending.

Another result that stands out is that differences between nonpolar cyHex, intermediate-polarity Et_2O, and highly polar MeCN are exclusively due to a variation in the zeroth-order contributions, whereas the first-order contributions are virtually identical for all three solvents. This finding holds for all of the molecules investigated in this work and is independent of the level of QM theory employed. The mean absolute deviation between the first-order terms for the same molecule in different solvents is smaller than 4 meV for the complete data set at the ADC(2)/ptSS-PCM level of theory.

Considering the large variation of the single terms contributing to the first-order correction shown in Figure 4,

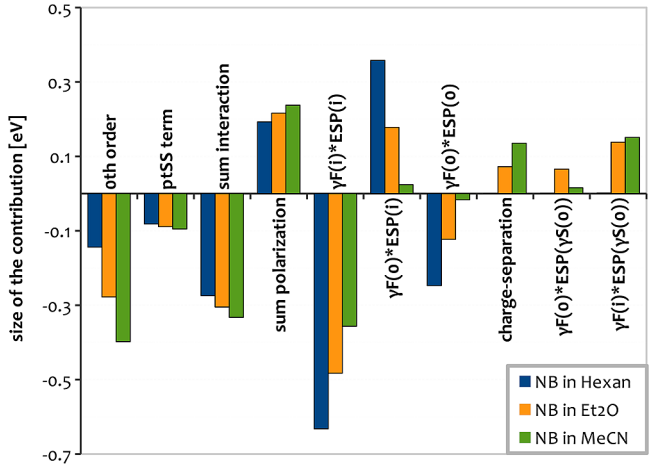

Figure 4. Breakdown of the first-order contributions into the single terms (eq 16) and the sums of all interaction and polarization term for nitrobenzene in hexane, diethyl ether, and acetonitrile. Despite large differences in the separate terms, the final first-order corrections are virtually identical for all three solvents.

the similarity of the first-order contributions is even more remarkable. Obviously, a meaningful evaluation of the latter should involve gas-phase to solvent shifts. However, the small variation in the optical dielectric constant among typical solvents (n^2 = 1.75−2.25) causes the differences in calculated first-order terms to be too small for a meaningful evaluation. If an evaluation of zeroth-order terms is desired, e.g., for the comparison of PTE and PTD schemes in the next section, a comparison involving solvents of different polarity is advisible.

D. Basis Set Dependence. We recalculated solvent shifts for nitrobenzene in cyHex, Et_2O and MeCN at the ADC(2)/ptSS-PCM and ADC(2)/ptLR-PCM levels of theory using the

DOI: 10.1021/jp511163y
J. Phys. Chem. A 2015, 119, 5446−5464

(aug-)cc-pVDZ and (aug-)cc-pVTZ basis sets. Examining the results shown in Figure 5, one finds that the ptLR terms

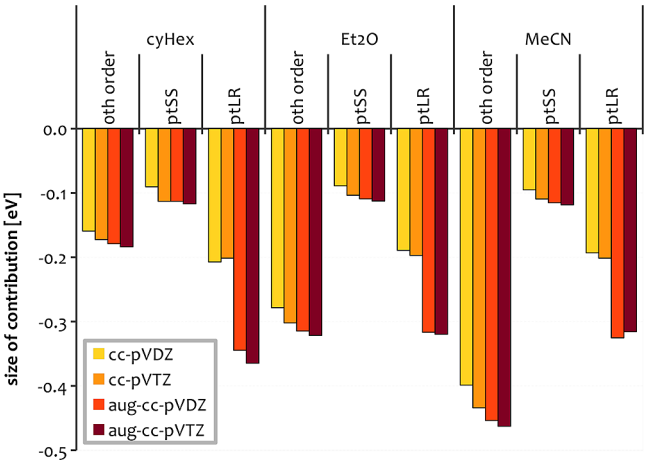

Figure 5. Components of the calculated solvent shifts with ADC(2)/ptSS- and ptLR-PCM for the cc-pVDZ, aug-cc-pVDZ, cc-pVTZ, and aug-cc-pVTZ basis sets.

increase by more than 65% (0.3 eV vs 0.2 eV) for the augmented basis sets. The ptSS-corrections, on the contrary, are less affected by the augmentation (+20%, 0.11 eV vs 0.09 eV) but show a larger increase for the cc-pVTZ basis (15% increase for ptSS vs 4% increase for ptLR).

Also the zeroth-order contributions of the shifts exhibit a basis set dependence. The augmentation of the cc-pVDZ basis causes an increase of about 13% (0.18 eV vs 0.16 eV for cyHex, 0.40 eV vs 0.45 eV for MeCN), whereas the triple-ζ basis yield zeroth-order shifts are about 8% bigger than those obtained with the double-ζ basis. For the ptSS approach, the differences between the medium (cc-pVTZ, aug-cc-pVDZ) and largest (aug-cc-pVDZ) basis sets are smaller, which indicates a convergence of the results.

Ultimately, the complete shifts obtained with the largest aug-cc-pVTZ for the ptSS approach are increased by 18% (0.43 eV vs 0.37 eV for Et_2O) compared to the smallest cc-pVDZ. Very similar changes are obtained for cyHex (20%) and MeCN (18%). For the ptLR approach, the differences between cc-pVDZ and aug-cc-pVTZ are even larger and there is more variation among the solvents. For cyHex, the shifts increase by 50% (0.55 eV vs 0.37 eV), for Et_2O the increase is 37% (0.64 eV vs 0.47 eV) and for MeCN it is 32% (0.78 eV vs 0.59 eV).

The reason for this pronounced basis-set dependence of the results is presumably the charge-transfer character of the excited states under investigation. Due to a surplus of negative charge located at the nitro group in the excited states, the description of the excited states profits tremendously from the introduction of diffuse functions and the additional flexibility of a triple-ζ basis. This is corroborated by the calculated gas-phase excitation energies and their agreement with the experimental values. At the ADC(2) level of theory, the difference between calculated and experimental excitation-energies decreases from +0.66 eV (cc-pVDZ) to +0.23 eV (aug-cc-pVTZ), whereas ADC(3) is off by +0.37 eV with cc-pVDZ and quantitative with aug-cc-pVTZ (+0.05 eV). Hence, for a reasonable description of the states and their solvatochromism, the use of larger basis sets is advisible. This would, however, lead to prohibitively expensive calculations at the ADC(3) level of theory. Hence, to retain comparability between the methods, the cc-pVDZ basis was used throughout this work and the results from this basis-set study will be considered in the discussion.

E. PTE vs PTD. To evaluate the PTD correction, calculated solvent shifts for a selection of molecules from the first (exclusively electrostatic) subgroup of the xBDSM set in cyHex,

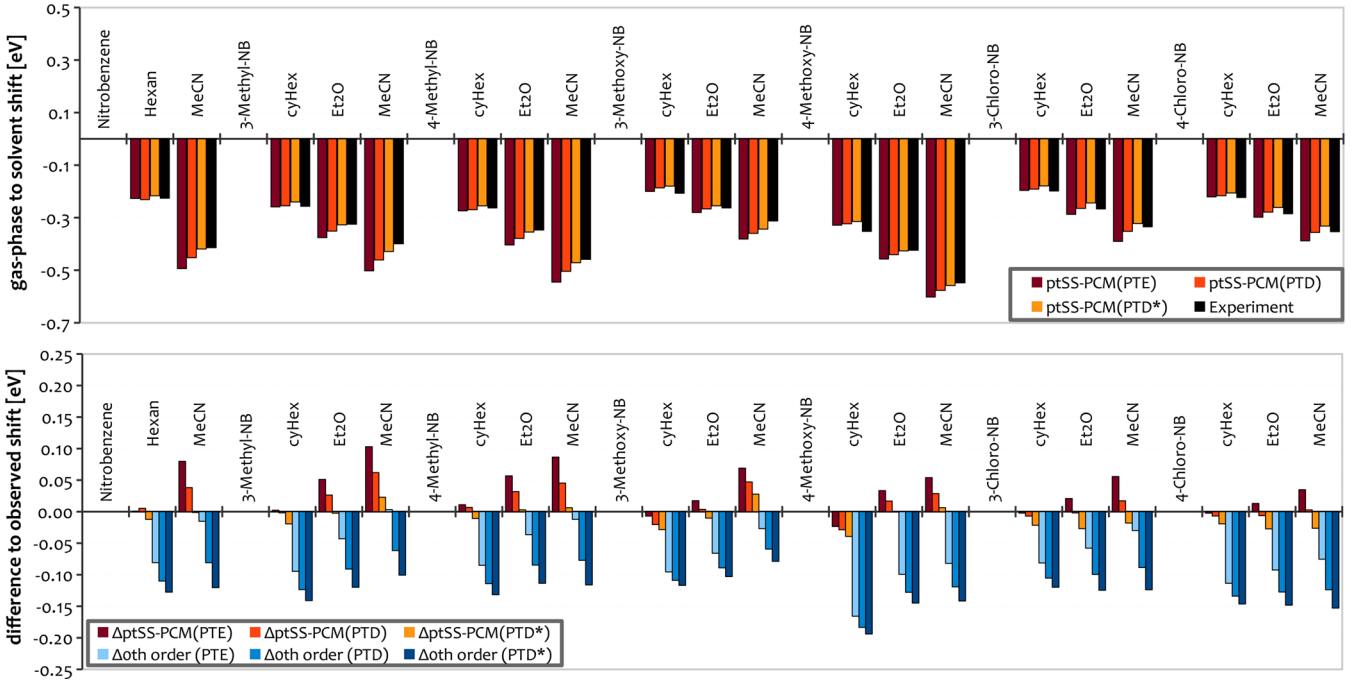

Figure 6. Top: experimental and calculated solvent shifts for a selection of molecules in the exclusively electrostatic subgroup of xBDSM. Solvent shifts are computed at the ADC(2)/ptSS-PCM level of theory with the PTE, PTD, and scaled PTD* approaches. Bottom: differences between experimental and calculated solvent shifts for the PTE, PTD, and scaled PTD* approaches including also the zeroth-order terms.

DOI: 10.1021/jp511163y
J. Phys. Chem. A 2015, 119, 5446−5464

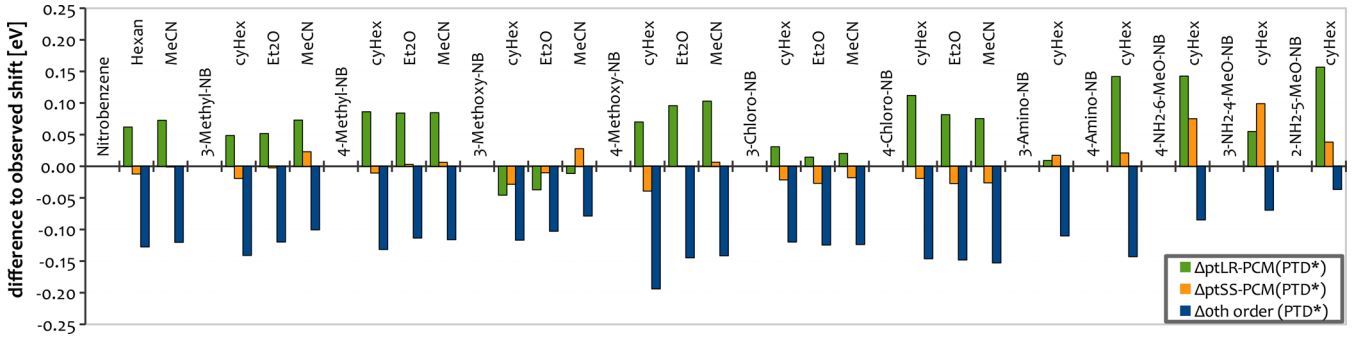

Figure 7. Differences between calculated and experimental solvent shifts at the ADC(2) level of theory using either the ptSS or ptLR scheme, in conjunction with the empirically scaled PTD* zeroth-order contribution.

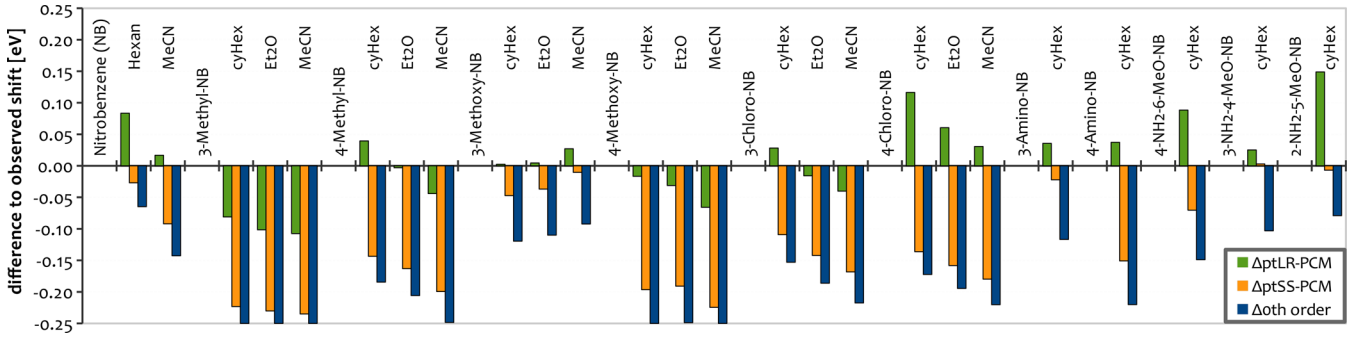

Figure 8. Experimental and calculated solvent shifts for the exclusively electrostatic subgroup of xBDSM calculated at the ADC(1)/ptSS-PCM and ADC(1)/ptLR-PCM levels of theory.

Et_2O, and MeCN are compared to the respective experimental values. The calculations were carried out at the ADC(2) and ADC(3/2) levels of theory using the ptSS-PCM approach, and results are shown in Figure 6 for ADC(2) and Figure 9 for ADC(3/2). We find that solvent shifts computed using the PTE scheme are overestimated by an amount proportional to the solvent polarity. On a molecular level, this systematic error can be traced back to the poor description of the ground state at the Hartree−Fock level of theory, which is the level at which the ESP of the solute is computed in the PTE approach. In particular, the dipole moment of the nitrobenzylic moiety is overestimated by about 20% at the HF level as compared to the unrelaxed MP2 dipole moment. For polar solvents that exhibit a large nuclear component of the polarization, this error gives rise to a systematic overestimation of the solvent shifts as the slow component of the ground-state polarization enters the calculation of the excitation energies in zeroth order. For unpolar solvents there is a similar overpolarization, but it only affects the fast component of the ground-state polarization, whose interaction with the excited state is, however, subtracted in the first-order terms (eq 16, second term in the first line).

As supposed in section IIID, the PTD corrections systematically reduce the error but do not eliminate it quantitatively. To compensate for this empirically, we have scaled the zeroth-order PTD correction by an empirical factor of 1.6, such that the systematic error is minimized as shown in Figure 6. We denote this scaled-PTD approach as PTD*.

For ADC(3/2) already the unscaled PTD correction overcompensates the error introduced by the HF-reaction field (Figure 5). Apparently, the optimal scaling factor is different for ADC(3/2). Using the same procedure as for ADC(2), one finds that a scaling factor of 0.5 largely eliminates the systematic error. Hence, in the following, a scaling factor of 0.5 will be used for the ADC(3/2)/ptSS-PCM(PTD*) approach.

The reason for the differences between the PTD approach for ADC(2) and ADC(3/2) are presumably the formal inconsistencies of the ADC(3/2)/ptSS-PCM(PTD) scheme, which combines a PTD correction calculated for the MP(2) ground state with correction terms evaluated with ADC(3/2) excited-state densities.

F. ptSS and ptLR with ADC and TDDFT. To compare the accuracy and investigate the relation of the perturbative, state-specific corrections and linear-response-type corrections, solvent shifts for the exclusively electrostatic subgroup at the ADC(1), ADC(2), ADC(3/2, and TD-DFT/LRC-ωPBE levels of theory have been calculated. For the isolated bright excited states of the monosubstituted nitroaromatics, the results of the ptLR corrections are quite close to the original, self-consistent LR formalism.[69] In the case of nitrotoluene, for example, the self-consistent LR solvent shifts are 0.185, 0.251, and 0.325 eV in cyHex, Et_2O, and MeCN, respectively, whereas the same shifts computed with our ptLR approach are 0.186, 0.259, and 0.325 eV.

1. Results for ADC(2). ADC(2) results using either the ptLR or ptSS scheme are shown in Figure 7. In general, the accuracy of the solvent shifts calculated at the ADC(2)/ptSS-PCM-(PTD*) level of theory is remarkable. Most errors are well below 0.05 eV, with a mean error of 2 meV, and the largest deviation is 0.08 eV. The root-mean-square deviation (RMSD) is 32 meV, which is most likely comparable to the experimental uncertainty. This agreement demonstrates that our first-order treatment of the fast solvent response is sufficient. The improved accuracy of the PTD approach falls into place from a theoretical point of view, because all corrections are based on densities computed at a consistent order of perturbation theory,

DOI: 10.1021/jp511163y
J. Phys. Chem. A 2015, 119, 5446−5464

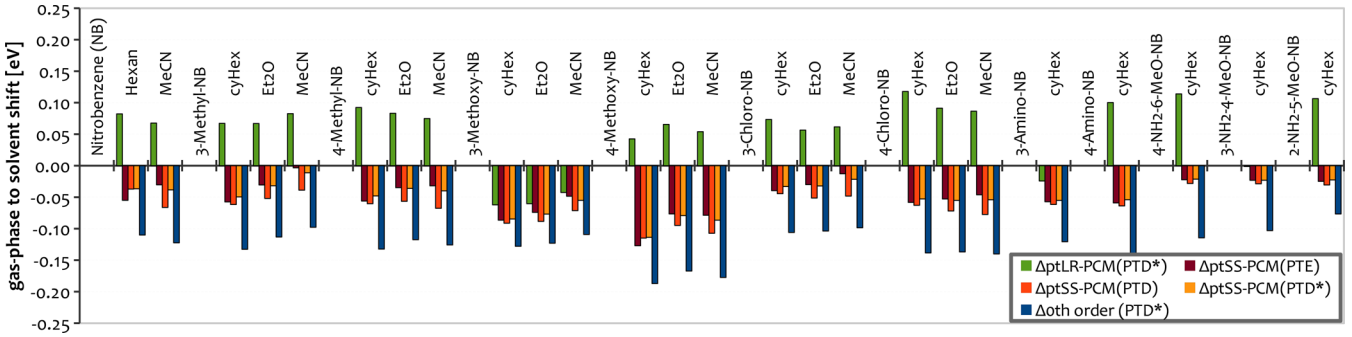

Figure 9. Differences between experimental and calculated solvent shifts for the exclusively electrostatic subgroup of xBDSM computed at the ADC(3/2)/ptSS-PCM and ADC(3/2)/ptLR-PCM levels of theory in combination with the PTE, PTD and PTD* schemes.

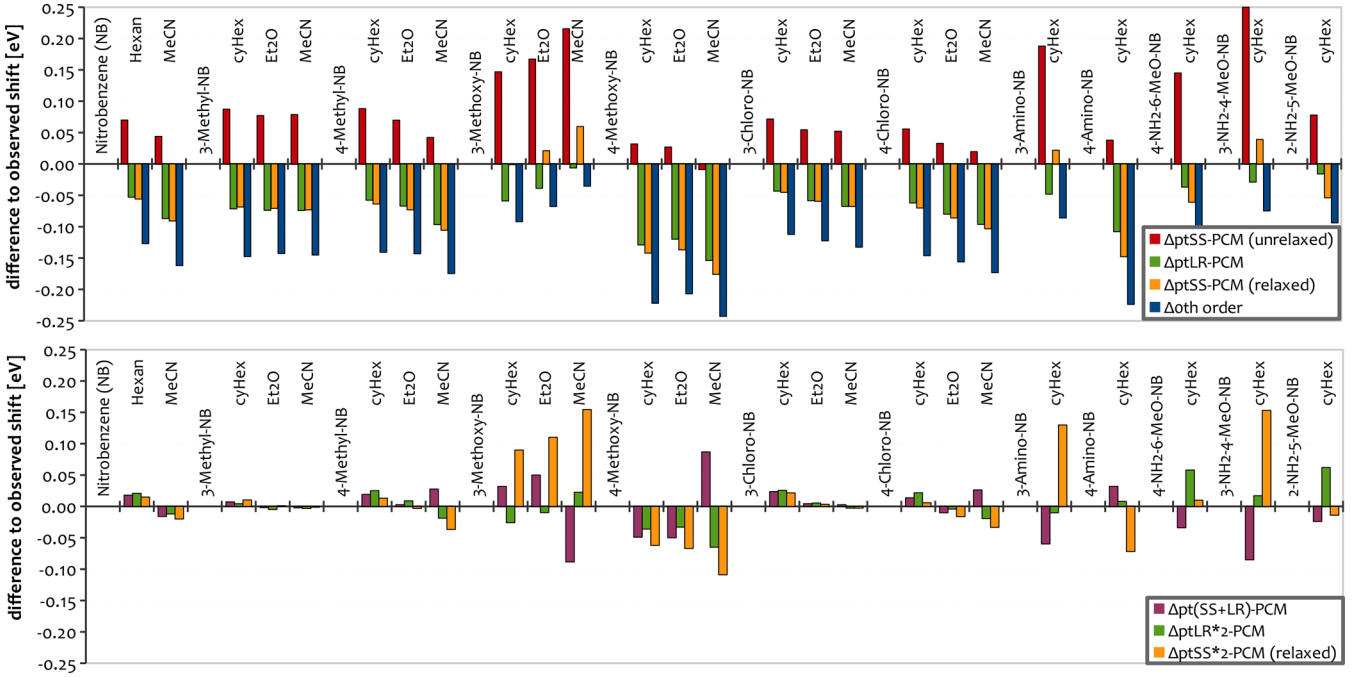

Figure 10. Top: differences between calculated and experimental solvent shifts for ptSS and ptLR approaches as well as the zeroth-order contribution at the LRC-ωPBE/ptSS-PCM and/ptLR-PCM levels of theory. Bottom: differences between calculated and experimental solvent shifts for the empirically scaled ptSS*2 and ptLR*2 approaches as well as the combined pt(LR+SS) approach.

whereas for the PTE approach, excitation energies and correction terms obtained at second-order are combined with a solvent field obtained for a first-order (HF) ground-state wave function.

Considering the increase of the solvent shifts observed for larger basis sets (section VD), the very good agreement observed here benefits from some error compensation. For the aug-cc-pVTZ basis set, one would presumably observe a slight but systematic overestimation of the solvent shifts.

The combination of ADC(2)/PCM(PTD*) zeroth-order energies with the ptLR correction is not nearly as accurate as the ptSS approach. The shifts are systematically overestimated (mean error = 58 meV, MAD = 73 meV, RMSD = 81 meV), and in three of the examples the zeroth-order correction actually lies closer to (or as close to) the experimental result than the full ptLR result. Moreover, the accuracy of the ptLR results seems to depend on the character of the excited state: shifts obtained for states that are related to the 2 A_1 (HOMO−1 → LUMO) state of NB are generally too large, whereas shifts are accurate or slightly underestimated for states related to the 1 B_1 (HOMO → LUMO) transition, as in 3-methoxy-NB and 3-amino-NB.

2. Results for ADC(1). ADC(1) results (Figure 8) are in sharp contrast to those obtained using ADC(2). For ADC(1), the ptSS correction terms are systematically too small (mean error = −127 meV, MAD = 127 meV, RMSD = 148 meV), whereas the ptLR-PCM is balanced and much more accurate than for ADC(2) (mean error = 10 meV, MAD = 50 meV, RMSD = 63 meV). In general, the average deviation in the solvent shifts at the ADC(1)/ptLR-PCM level of theory is much smaller than for ADC(2)/ptLR-PCM(PTD*) and rather compares to that of ADC(2)/ptSS-PCM(PTD*). Surprisingly, the deviations in the shifts calculated at the ADC(1)/ptLR-PCM level of theory are systematic with respect to solvent polarity but follow an inverse pattern (smaller shifts for polar solvents) as compared to those observed for ADC(2) in combination with the PTE approach.

3. Results for ADC(3/2). Surprisingly, the accuracy of the shifts calculated with ADC(3/2) and the ptSS-PCM(PTD*) scheme does not improve compared to ADC(2). On the contrary, the shifts calculated with ADC(3/2)/ptSS-PCM-

DOI: 10.1021/jp511163y
J. Phys. Chem. A 2015, 119, 5446−5464

(PTD*) are systematically too low (mean error = −49 eV, MAD = 49 meV, RMSD = 54 meV) (Figure 9). A detailed analysis and comparison of zeroth- and first-order contributions to those obtained for ADC(2) reveals that this is mainly due to smaller ptSS correction terms (77 meV, on average, versus 123 meV), whereas the zeroth-order contributions (PTD*) are very similar (mean deviation = −126 meV versus −120 meV). Probably due to fortuitous error compensation, the ptSS corrections yield a better agreement with the experiment in combination with ADC(3/2) zeroth-order energies obtained with the PTE scheme (mean error = −47 meV, MAD = 47 meV, RMSD = 52 meV). The differences to ADC(3/2)/ptSS-PCM(PTD*) are, however, negligibly small.

Regarding the very systematic underestimation of the solvent shifts observed for ADC(3/2)/ptSS-PCM, one should bear in mind the basis-set dependence of the shifts. Obtained with augmented and/or triple-ζ basis sets, the solvent shifts might be about 20% larger, which would yield something much closer to quantitative agreement with experiment.

The ptLR corrections in combination with ADC(3/2)/PCM(PTD*) zeroth-order energies yield consistently too large solvent shifts (mean error = 63 meV, MAD = 71 meV, RMSD = 81 meV). As in the case of ADC(2)/ptLR-PCM, the results of the ptLR approach seem to depend on the character of the excited state. Whereas the shifts are overestimated for those states related to the 2 A_1 state of nitrobenzene, the shifts for the 1 B_1 cases (3-methoxy-NB and 3-amino-NB) are slightly too low.

4. Results for TD-DFT. The TD-DFT/LRC-ωPBE results are different from any of the ADC/PCM combinations, in particular regarding the ptLR approach. The shifts predicted by the latter are systematically too *small* (mean error = −69 meV, MAD = 69 meV, RMSD = 77 meV). The same applies to the TD-DFT/ptSS-PCM corrections (mean error = −64 meV, MAD= 76 meV, RMSD = 86 meV). Regarding the very similar underestimation of the sovlent shifts with the ptSS approach for ADC(1), one may suggest that first-order excited-state densities are not accurate enough for ptSS calculations, and that at least second-order excited-state densities are needed to obtain accurate first-order corrections to the solvent shifts with the ptSS approach.

For TD-DFT, the first-order terms of ptLR and ptSS approaches are virtually identical for most of the molecules in the xBDSM set. The cases where they differ include 3-methoxy-NB and 3-amino-NB (excitations related to the 1 B_1 state of nitrobenzene), along with the *para*-substituted isomers of 3-amino-NB (Figure 10). The connection between these cases are the strong electron-pushing substituents ($-NH_2$ and −OMe), and as such one would expect the largest degree of CT character in these cases; this offers a hint that CT character may explain differences between the ptSS and ptLR approaches. Considering the much better agreement with experiment for the ptLR approach (see below), one may conclude that even with range-separated functionals like LRC-ωPBE, and a systematic adaptation of the range-separation parameter, the excited-state density is not properly described when there is significant CT character. A recent investigation of this issue can be found in ref 30.

Because the deviations from the experiment are systematic underestimation, the first-order terms can be scaled up pragmatically. Surprisingly, with a scaling factor of exactly 2.0, the ptLR*2-PCM approach yields the most accurate description of the solvatochromic shifts in this work (mean error = 1 meV, MAD = 21 meV, RMSD = 28 meV), with virtually no mean deviation and a maximum error of only 60 meV (Figure 10). Although scaling with the same factor also improves the ptSS results dramatically, the resulting ptSS*2-PCM approach is not nearly as accurate as the scaled ptLR approach. In particular, one finds a large overestimation of the shifts for the CT examples, for which the ptSS and ptLR first-order terms differ (mean error = 10 meV, MAD = 45 meV, RMSD = 68 meV, with several large errors of about 0.15 eV). Motivated by previous work,[21] and the idea that the state-specific and linear-response approaches describe different physical effects, the combination of first-order terms of the ptSS and ptLR approaches has also been studied. Indeed, also this pt(SS+LR) approach improves the results significantly but is not as accurate as the scaled ptLR approach (mean error = −4 meV, MAD = 32 meV, RMSD = 47 meV).

5. Discussion of the Results. A statistical analysis of the error for the investigated QM/PCM methods, as applied to the electrostatically dominated subset of xBDSM, is given in Table 2 and plotted in Figure 11. The most accurate methods are clearly TDDFT/ptLR*2-PCM, TDDFT/pt(SS+LR)-PCM, and ADC(2)/ptSS-PCM(PTD*), and if the basis-set dependency is considered, also ADC(3/2)/ptSS-PCM.

Table 2. Statistical Errors for the Electrostatically-Dominated Subset of the xBDSM Data Set

method	error/meV		
	mean	MAD	RMSD
	Zeroth Order		
LRC-ωPBE	−141	141	149
ADC(1)	−185	185	198
ADC(2) (PTE)	−67.3	67.7	77.5
ADC(2) (PTD)	−101	101	105
ADC(2) (PTD*1.6)	−120	120	124
ADC(3/2) (PTE)	−111	111	114
ADC(3/2) (PTD)	−140	140	142
ADC(3/2) (PTD*0.5)	−126	126	128
	ptLR-PCM		
LRC-ωPBE	−70.0	70.0	77.3
LRC-ωPBE (ptLR*2)	0.9	20.7	27.5
ADC(1)	9.5	50.1	63.1
ADC(2) (PTD*1.6)	66.4	73.4	83.0
ADC(3/2) (PTD*0.5)	55.8	71.1	75.8
	ptSS-PCM		
LRC-ωPBE	−65.6	76.4	86.0
LRC-ωPBE (ptSS*2)	10.0	45.2	67.6
ADC(1)	−126.5	−126.7	148.1
ADC(2) (PTE)	38.9	41.7	52.9
ADC(2) (PTD)	22.0	27.9	37.8
ADC(2) (PTD*1.6)	2.1	23.2	31.9
ADC(3/2) (PTE)	−48.7	48.7	55.3
ADC(3/2) (PTD)	−63.1	63.1	67.1
ADC(3/2) (PTD*0.5)	−48.5	48.5	54.1
	pt(SS+LR)-PCM		
LRC-ωPBE	−3.5	30.2	40.4

First, it bears pointing out that our perturbative ptLR corrections are formally *not* identical to the self-consistent LR-PCM formalism described in the literature.[22,21] Nevertheless, for nitrotoluene our ptLR scheme affords results that are essentially identical to those obtained using the self-consistent LR-PCM procedure as implemented in Q-Chem.[69]

DOI: 10.1021/jp511163y
J. Phys. Chem. A 2015, 119, 5446−5464

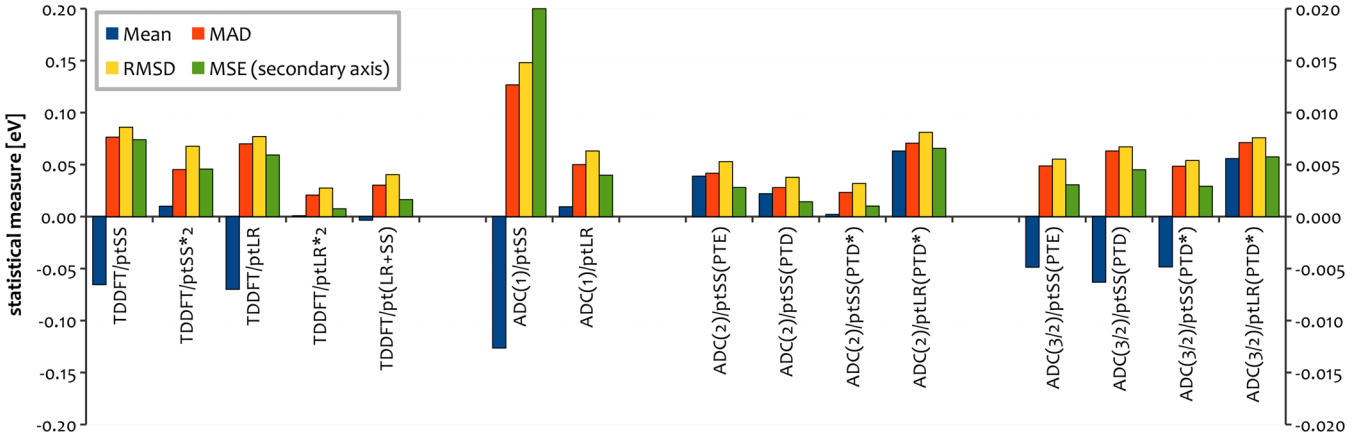

Figure 11. Statistical errors in various QM/PCM schemes as applied to the electrostatically dominated subset of xBDSM. For the sake of completeness, the results for the scaled ptSS*2 and combined pt(SS+LR) approaches in combination with TD-DFT are given.

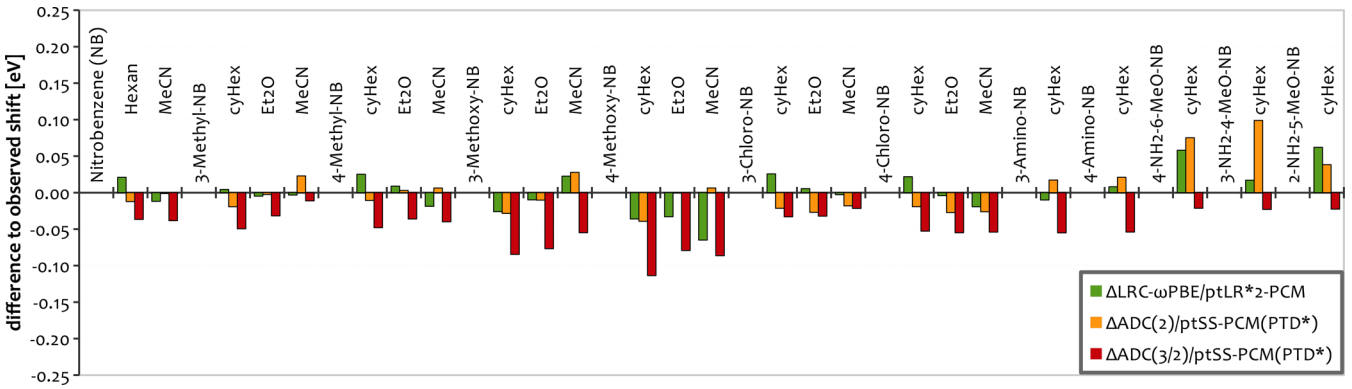

Figure 12. Direct comparison of the errors of the most accurate QM/PCM combinations for the first xBDSM subset.

Let us begin the discussion with an interpretation of our results regarding the relation of the ptLR and ptSS formalisms. The zeroth-order (static polarization) energies are identical in both cases, but the first-order terms are generally regarded as describing different physical phenomena. Specifically, the first-order ptSS contribution is associated with the dynamical response of the fast component of the polarization, whereas the first-order LR correction has been suggested to relate to excitonic coupling[21] or dispersion effects.[51,70] We find that for the case of TD-DFT, the ptLR and ptSS corrections (as formulated here) afford similar values in cases where the solvatochromic shift is dominated by electrostatic effects. However, the relation between the ptLR and ptSS corrections also depends on the underlying QM level of theory. For ADC(2) and ADC(3/2), the ptLR corrections are about twice as large as the ptSS corrections (mean 0.19 eV vs 0.11 eV for ADC(2), 0.18 eV vs 0.08 eV for ADC(3/2)).

With respect to the accuracy of the ptSS and ptLR approaches for the first xBDSM subset, there are only negligible differences if one compares the best-performing QM/PCM combinations (Figure 12). The results indicate that the ptSS correction is more sensitive with respect to the level of theory, which is to say, more sensitive to the quality of the excited-state densities. Taking into account the basis-set dependence of the shifts, the accuracies of the ptSS-PCM combinations with ADC(2) and ADC(3/2) are presumably very similar. In combination with the CIS-related ADC(1) and TD-DFT, however, one finds a systematic underestimation of the solvent shifts.

For the ptLR-PCM approach, the exact opposite is the case. It affords the most accurate solvatochromic shifts when combined with TD-DFT (upon empirical scaling by a factor of 2.0), and also with ADC(1) the predicted shifts are balanced and accurate (without a scaling). For ADC(2) and ADC(3/2), however, the ptLR correction terms are too large to suite the zeroth-order excitation energies, which are closer to the experimental shifts for ADC(2) and ADC(3/2) (mean deviation about −0.125 eV) than for ADC(1) (mean deviation −0.155 eV). The ptLR corrections are, however, very similar for ADC(1) (mean 0.19 eV), ADC(2) (mean 0.19 eV), and ADC(3/2) (0.18 eV).

Despite these differences between the ptSS and ptLR corrections, we conclude that the electrostatic information relevant to the fast solvent response seems to be encoded in the *transition density*, not just in the excited-state density. As such, the ptLR and the ptSS formalisms constitute different ways to extract this information and translate it into an energy correction. If the ptLR formalism would indeed describe an entirely different physical effect, it should not give rise to any sizable contribution for the nitroaromatic compounds, whose solvatochromism is apparently well-described with the purely electrostatic ptSS-PCM approach.

A recent series of articles of Plasser et al.,[54,55] in which they presented a detailed analysis of the density matrices occurring within the ADC computational framework might help to guide this discussion. They demonstrated that the transition density matrix simply represents the orbital transitions contained in the ADC response vector whereas the excited-state densities are

DOI: 10.1021/jp511163y
J. Phys. Chem. A 2015, 119, 5446−5464

characterized by additional contributions deriving from secondary orbital relaxation effects, which are present whenever significant charge shifts occur.[55] With these results in mind, one may suggest that the essential difference between ptLR and ptSS correction is that the ptSS correction terms do include orbital relaxation via the respective densities, whereas the former, transition-density based ptLR corrections do not. This is in line with the better agreement and much more systematic errors of the ptSS-approach in combination with ADC(2) and ADC(3/2). Because for the latter, the relaxation effects are also included in the zeroth-order energies, the ptLR correction terms are just too large. Hence, for correlated higher-order methods, the ptSS approach should be preferred over the ptLR approach.

For first-order methods like TD-DFT or ADC(1), which hardly include any orbital relaxation in the zeroth-order excitation energies, the ptLR-approach constitutes a shortcut to obtain the response of the solvent polarization that circumvents the explicit calculation of the excited-state wavefuntion. From this perspective, also the agreement of ptLR and ptSS-terms for the linear-reponse method TD-DFT falls into place. A drawback of the ptLR-PCM approach is due to the mathematical structure of the transition density as a product of electron and hole orbitals. For CT excitations associated with large electron−hole separation the transition density becomes zero and so do the ptLR correction terms. As a concrete example, we choose the lowest CT excitation of the C_2H_4/C_2F_4 complex[24] (Figure 13). Obviously, the transfer of

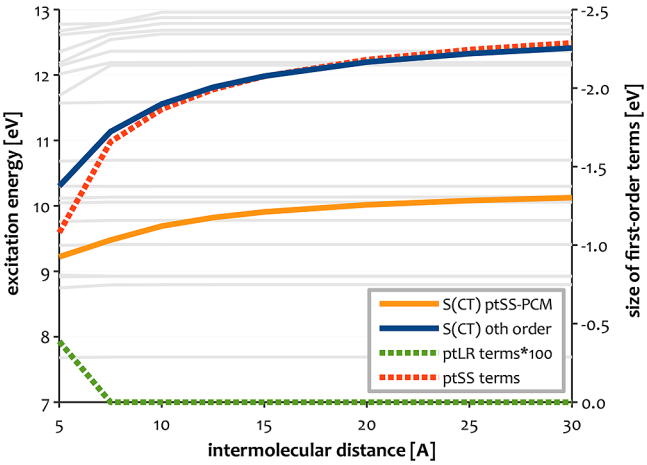

Figure 13. Zeroth- and first-order energy of the electron-transfer excitation of the C_2H_4/C_2F_4 complex in MeCN, computed at the ADC(2)/ptSS-PCM(PTD) and ADC(2)/ptLR-PCM levels of theory. The magnitude of the first-order ptLR and ptSS terms can be read from the vertical axis on the right. As the intermolecular separation increases, only the ptSS approach affords a physically correct description, whereas the fast solvent response vanishes at the ptLR level.

an electron should give rise to a pronounced response of the fast component of the polarization because two full charges are created in the process, but due to negligible overlap between initial and final orbitals, the transition density for this excitation vanishes and so does the ptLR correction. In this and comparable situations, only the ptSS approach affords a physically correct description.

G. Examples Involving Hydrogen Bonds. The PCM describes only the (long-range) electrostatic interaction with the bulk solvent, not specific interactions such as hydrogen bonds. In the previous section, the accuracy of the ADC(2)/ptSS-PCM(PTD*) and LRC-ωPBE/ptLR*2-PCM approaches has been established to be ∼50 meV for cases in which the solvatochromic shift is dominated by electrostatic effects. Here, we examine how these approaches behave for cases in which hydrogen bonding affects the excitation energy and how this can be included in the model by adding few explicit solvent molecules. It should be mentioned that this approach is a pragmatic attempt to include explicit interactions into the PCM description, and the results should be taken with a grain of salt. In particular, the solvent-relaxed geometries of this complexes are essentially meaningless.

Consider the moderately strong H-bonding case of *para*-nitroaniline (pNA). Already for the weakly Lewis-acidic solvents Et_2O and MeCN, inclusion of explicit solvent molecules has a notable influence onto the excitation energy (Figure 14), as coordination to the solvent stabilizes the

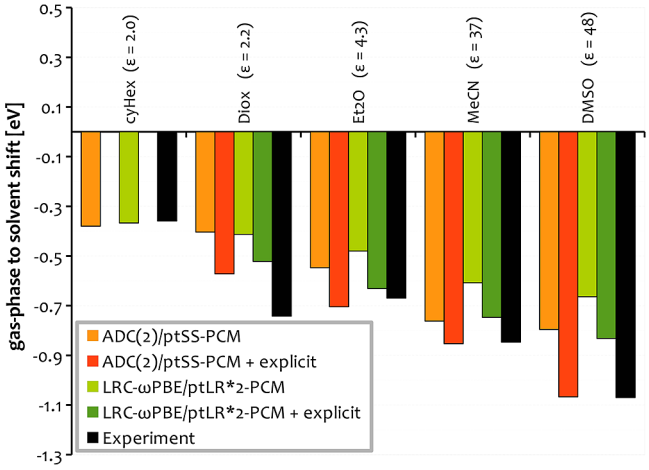

Figure 14. Experimental and calculated solvent shifts for *para*-nitroaniline (4-amino-NB) at the ADC(2)/ptSS-PCM(PTD*) and LRC-ωPBE/ptLR*2-PCM levels of theory. Results are shown both with and without a single explicit solvent molecule in the QM region.

positive charge at the amine that is created in the excited state, and thus lowers the excitation energy. This effect is even more pronounced for the nonpolar, but more Lewis-basic solvent dioxane (ϵ = 2.25). The excitation energy in dioxane (3.50 eV) is actually closer to that observed in the polar solvent MeCN (ϵ = 36.7, 3.39 eV) than it is to the excitation energy in cyclohexane (ϵ = 2.03, 3.88 eV). Thus, the influence of hydrogen bonding to pNA in dioxane is actually larger than the effect of the bulk electrostatic interactions. Inclusion of one explicit solvent molecule within the QM region does generally move the calculated solvent shifts in the right direction, as shown in Figure 14. In particular with ADC(2)/ptSS-PCM(PTD*), the inclusion of a single solvent molecule restores the accuracy quantitatively for all cases but dioxane.

For cases such as charged chromophores in water that exhibit very strong, ionic hydrogen bonds, calculation of reliable solvent shifts is more involved. Especially in cases where the chromophore has more than one H-bonding site, one may need to sample over conformations of the explicit solvent molecules.[71] In our experience, a practical approach is to (1) successively include water molecules at one H-bond donor or acceptor site after another, (2) optimize the structure with a method appropriate for the description of intermolecular

DOI: 10.1021/jp511163y
J. Phys. Chem. A 2015, 119, 5446−5464

interactions (e.g., B2-PLYP+D3) using a PCM, and (3) calculate the excitation energies and see if and how the results converge with the number of explicit solvent molecules.

Following this protocol, we investigated the vacuum-to-water solvatochromic shifts in 4-nitrophenolate (4-NP) and 4,4′-nitrophenylphenolate (44-NPP), which differ (−0.08 eV vs +0.87 eV, respectively)[68] despite the similar structures of the two molecules. We successively added up to four water molecules, two each at the phenolate and nitro groups, optimized the structures, and then calculated the excited states at the ADC(2)/ptSS-PCM(PTD) and LRC-ωPBE/ptLR*2-PCM levels of theory (Figure 15).

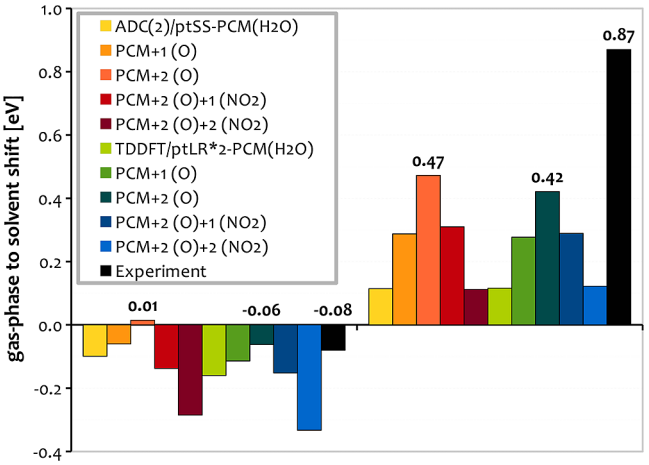

Figure 15. Experimental and calculated solvent shifts for 4-nitrophenolate (on the left) and 4-(4-nitrophenyl)phenolate (on the right) at the ADC(2)/ptSS-PCM(PTD) and LRC-ωPBE/ptLR*2-PCM levels of theory with up to two explicit water molecules at the phenolate group and up to two more at the nitro group.

Despite the apparent presence of strong ionic hydrogen bonding, both methods yield a reasonable, qualitatively correct estimate of the observed solvent shifts even without explicit solvent molecules. Whereas the introduction of explicit water molecules to the phenolate improves the agreement with the experiment, additional water molecules at the nitro group decrease the accuracy of the model. One may conclude that the explicit interactions of the solvent with the ionic phenolate are much stronger and thus more important compared to those with the nitro group. This is corroborated by the fact that nitrobenzene itself is, despite its large dipole, virtually insoluble in water. Due to an apparently imbalanced explicit solvation scheme, none of the methods yields a quantitative answer for both molecules.

All together, one may conclude that ADC(2)/ptSS-PCM is more robust with respect to the introduction of explicit solvent molecules. In particular, for the examples involving 4-nitroaniline, the results for the explicitly solvated systems are as accurate as for the cases without explicit interactions.

H. Nonelectrostatic Examples. The lowest electronic transitions in pyridine as well as the lowest two in benzofuran and coumarin exhibit only a very small (or zero) solvatochromic shift among the gas phase, hexane, and acetonitrile. This makes these cases very different from the electrostatically dominated examples discussed thus far. To investigate how the best-performing QM/PCM combinations work for these cases, we calculated solvent shifts at the ADC(2) and LRC-ωPBE levels of theory in combination with the ptSS-PCM and ptLR-PCM approaches. For ADC(2), we used PTD zeroth-order energies and for TD-DFT we used the empirically scaled ptSS*2 and ptLR*2 schemes.

Inspecting the results in Figure 16, we find a dramatic failure of the ptLR approach in the case of coumarin. Surprisingly, ADC(2) and TD-DFT deviate in opposite directions. An examination of the shifts reveals that in the case of TD-DFT, the large blue shift is due to the zeroth-order term (+0.23 eV in the case of MeCN), whereas the ptLR term only −0.003 eV. In contrast, ADC(2) yields a much smaller contribution in the zeroth-order terms in MeCN (0.04 eV for PTD, −0.09 eV for PTE), whereas the ptLR correction is very large (−0.61 eV). For the case of ADC(2), this failure of the ptLR approach is most certainly due to the perturbative charater of our ptLR approach, which neglects coupling elements between excited states. A preliminary investigation of this particular example using the self-consistent implementation of the LR formalism for ADC(2)/COSMO in Turbomole[21] revealed that, indeed, the predicted solvent shift is much smaller (<0.1 eV) than the one obtained here. At the TD-DFT level of theory, however, the problem is present already at the stage of the TD-DFT calculation. The ptSS formalism in combination with ADC(2) yields the most accurate predictions for these nonelectrostatic cases.

VI. CONCLUSIONS

We have presented the first systematic evaluation of two new, PCM-based corrections for vertical excitation energies by comparison to experimental gas-phase to solvent shifts. For this purpose, we composed the experimental benchmark data for solvatochromism in molecules (xBDSM) set including 44 gas-

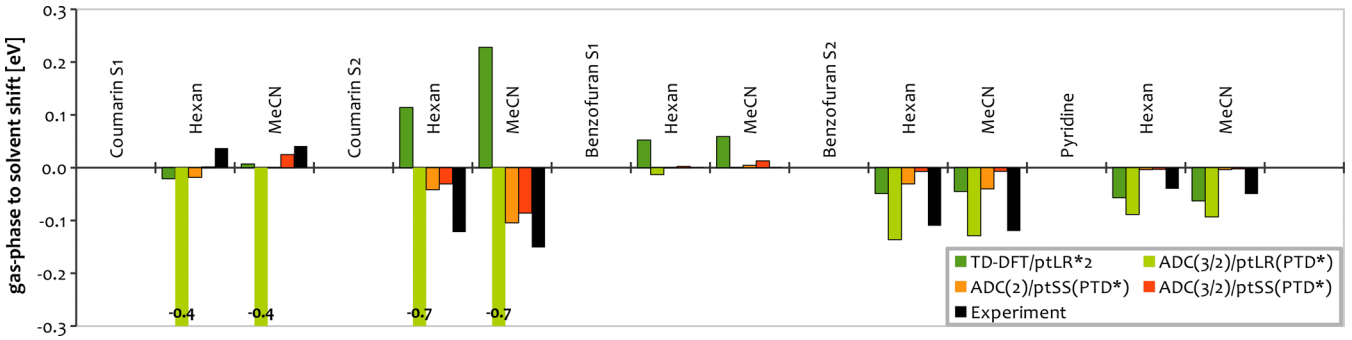

Figure 16. Experimental and calculated solvent shifts for the subset of nonelectrostatic examples, for ADC(2) and LRC-ωPBE calculations in combination with the ptSS and ptLR schemes.

DOI: 10.1021/jp511163y
J. Phys. Chem. A 2015, 119, 5446−5464

phase to solvent shifts for 17 molecules in three subgroups as well as the respective gas-phase and solvent-relaxed geometries. The first subgroup consists of examples whose solvatochromism is dominated by the bulk electrostatic interaction. The data points of this group can thus be accurately reproduced by the QM/PCM approach. In the second group, there are cases involving weak to strong hydrogen bonding. Its purpose is to study how hydrogen bonding affects the accuracy and how explicit solvent molecules in the QM subsystem can be used to overcome the shortcomings of pure PCMs. The third group consists of examples that exhibit very weak solvatochromism but have multiple bright excited states in close proximity. In this sense the third set is orthogonal to the former two and was used to demonstrate the limitations of our perturbative ptLR correction terms.

The presented PCM-based approaches are derived from the state-specific and linear-response formalisms. Termed perturbation-theoretical state-specific (ptSS)-PCM and perturbation-theoretical linear-response type (ptLR)-PCM, the correction terms depend solely on the zeroth-order excited-state or transition densities, respectively. Hence, the correction terms can just be added to the zeroth-order excitation energy, which is the same for both approaches. It can be obtained via an configuration-interaction (CI)-type calculation employing the polarized ground-state Hartree−Fock molecular orbitals as a reference. Consequently, the transfer of the approaches to other CI-type excited-state methods is straightforward.

By comparison to the xBDSM set, the performance of the ptSS-PCM and ptLR-PCM approaches was examined in combination with ADC of first to third order as well as TD-DFT/LRC-ωPBE. In doing so, we find that the ptLR-PCM method affords good accuracy in particular in combination with first-order methods. The ptSS-PCM approach, on the contrary, apparently requires accurate excited-state densities and in turn yields the most accurate results only in combination with correlated methods such as ADC(2) and ADC(3/2).

The statistically most accurate prediction of solvatochromism for the first xBDSM subset is obtained with the ptLR approach in combination with TDDFT/LRC-ωPBE (see Table 2 and Figure 11 for summaries of the error statistics for various methods). To achieve this accuracy, however, the ptLR corrections (first-order terms) have to be scaled by an empirically determined factor of 2.0 to eliminate a systematic underestimation (Figure 10). Although this scaling improves the results for all but one example in the xBDSM set, the generality of this scaling has to be questioned and should be investigated more thoroughly in the future. An almost as accurate model can be obtained for TD-DFT if the ptSS and ptLR correction terms are both added to the zeroth-order excitation energy. In contrast to the up-scaling of the ptLR terms, the combination of the ptSS and ptLR corrections can be physically motivated, if it is assumed that the two approaches describe different physical effects. However, this assumption is questionable regarding the almost identical first-order terms of the two methods for many of the examples.

For some of the examples in the third xBDSM subset, the TDDFT/ptLR*2 approach fails to yield even a qualitatively correct description. These are on the one hand coumarin, for which the zeroth-order excitation energies are by far too large, and on the other hand charge-transfer excitations with large electron−hole separation, for which the ptLR corrections become zero due to a vanishing transition-density.

The ptSS-PCM approach yields a very accurate description of solvatochromism in combination with the correlated ADC(2) and ADC(3/2) methods. This is true in particular for the PTD variants of the methods, in which the zeroth-order excitation energies are corrected for deficiencies in the HF solvation field (see sections IIID and VE). Although the agreement with ADC(2) is quantitative with the rather small cc-pVDZ basis set, the combination with ADC(3/2)/cc-pVDZ yields a systematic underestimation of the shifts. If, however, diffuse functions and/or larger triple-ζ basis sets are employed, the calculated shifts are increased by about 20% (see section VD), which would largely eliminate the systematic error for ADC(3/2) and in turn yield a systematic overestimation for ADC(2). Concerning the total excitation energies instead of just the solvent shifts, ADC(3/2)/ptSS-PCM(PTD*) is certainly the most accurate for the prediction of vertical excitation energies in solution in this work, in particular if larger basis-set (e.g., aug-cc-pVTZ) are employed.

For the H-bonded examples including explicit solvent molecules, ADC(2)/ptSS-PCM(PTD*) is more accurate than the scaled LRC-ωPBE/ptLR*2-PCM. Moreover, the ptSS-approach yields a physically sound description of solvatochromism in cases with large electron−hole separation and does not fail qualitatively for any of the examples studied in this work. For molecules in which the solvent shift is *not* dominated by electrostatic interactions, the PTE variant of ADC(2)/ptSS-PCM was more accurate. This is probably due the fact that the solvent reaction field is iterated to self-consistency alongside the ground-state density, and furthermore the differences between the HF and MP2 ground state are much smaller than for the nitroaromatics. In combination with TD-DFT and ADC(1) the ptSS correction terms are systematically too small, which was traced back to poor excited-state densities.

Concerning the relation of the linear-response and state-specific approaches, we conclude that both approaches describe essentially describe the same electrostatic effect (response of the fast component of the polarization to an electronic excitation) within the perturbative formulation presented here. The main difference being that the ptSS approach allows us to include orbital-relaxation effects via the respective excited-state densities, whereas the ptLR approach, on the contrary, does not. This was traced back to the fact that the transition density itself does, in contrast to the excited-state density, not contain any orbital relaxation effects, even if computed with correlated methods such as ADC(2) and ADC(3/2).[55]

Along this line of thought, the good agreement obtained with the ptLR approach in combination with first-order methods such as TD-DFT and ADC(1) falls into place. Neither ADC(1) nor TD-DFT include orbital relaxation effects in the excitation energies. Hence, the latter are consistent with the "unrelaxed" ptLR correction terms. For ADC(2) and ADC(3/2), whose excitation energies do contain orbital relaxation effects, the ptLR correction terms are too large. For these correlated methods, also the first-order corrections need to include orbital-relaxation effects, which can only be achieved via the ptSS approach in combination with proper excited-state densities. Hence, for correlated methods the ptSS-approach is required to obtain a balanced description of solvent effects. Because our implementation of ADC in combination with the ISR formalism offers a very efficient way to obtain accurate excited-state densities directly from the excited-state vectors, i.e., without the need to calculate the orbital response explicitly (section IIIF), the ptSS- corrections can be calculated at

DOI: 10.1021/jp511163y
J. Phys. Chem. A 2015, 119, 5446−5464

essentially no extra computational cost compared to the respective excitation energies.

For TD-DFT, on the contrary, the ptLR*2-PCM approach seems to be the most accurate, in particular for bright excited states with large charge-transfer character. For the latter, the ptLR and ptSS correction terms differ significantly, whereas the scaled ptLR*2-PCM approach consistently yields a slightly better agreement with the experimental values than the combination of both approaches pt(SS+LR) (section VF4). Hence, we suggest to use the scaled ptLR*2-PCM approach in combination with TD-DFT.

After all, one may question whether the xBDSM data set, which mainly consists of nitroaromatic compounds is as diverse as it should be to provide representative error estimates for various PCM approaches. Unfortunately, this lack of diversity is mainly due to the combined limitations of the experiments and the calculations, which place tight constraints on the size of molecules that can be computed (with ADC methods) and the types of chromophores that yield unambiguous experimental solvent shifts. It would be useful to expand the size of this data set in the future, in particular the third subset of non-electrostatic examples. Despite the limitation, this first systematic evaluation of PCM-based solvent models by comparison to the xBDSM set provided valuable insights in the relation between SS and LR formalisms, and uncovered unexpected differences between density-based and wave-function-based methods within a PCM framework. Additional insight can be obtained from a derivation that starts from basic electrostatics, as will be presented in a forthcoming paper.[20]

■ ASSOCIATED CONTENT

Supporting Information

Optimized gas-phase and solvent-relaxed geometries as well as the gas-phase to solvent shifts of the xBDSM data set, and energies for all QM/PCM combinations for all molecules. This material is available free of charge via the Internet at http://pubs.acs.org.

■ AUTHOR INFORMATION

Notes

The authors declare no competing financial interest.

■ ACKNOWLEDGMENTS

Work by Z.-Q.Y. and J.M.H. was supported by the U.S. National Science Foundation, under grant no. CHE-1300603. J.M.H. is a Camille Dreyfus Teacher-Scholar. J.-M.M. thanks the Heidelberg Graduate School for Mathematical and Computational Methods in the Sciences for funding and computer time and F. Plasser for helpful discussions on the topic of excited-state densities.

■ REFERENCES

(1) Tomasi, J.; Mennucci, B.; Cammi, R. Quantum Mechanical Continuum Solvation Models. *Chem. Rev.* **2005**, *105*, 2999−3093.
(2) Friesner, R. A.; Guallar, V. Ab Initio Quantum Chemical and Mixed Quantum Mechanics Molecular Mechanics (QM MM) Methods for Studying Enzymatic Catalysis. *Annu. Rev. Phys. Chem.* **2005**, *56*, 389−427.
(3) Senn, H. M.; Thiel, W. QM MM Methods for Biomolecular Systems. *Angew. Chem., Int. Ed. Engl.* **2009**, *48*, 1198−1229.
(4) Fedorov, D. G.; Kitaura, K. Extending the Power of Quantum Chemistry to Large Systems with the Fragment Molecular Orbital Method. *J. Phys. Chem. A* **2007**, *111*, 6904−6914.
(5) Gordon, M. S.; Fedorov, D. G.; Pruitt, S. R.; Slipchenko, L. V. Fragmentation Methods: A Route to Accurate Calculations on Large Systems. *Chem. Rev.* **2012**, *112*, 632−672.
(6) van der Kamp, M. W.; Mulholland, A. J. Combined Quantum Mechanics Molecular Mechanics (QM MM) Methods in Computational Enzymology. *Biochemistry* **2013**, *52*, 2708−2728.
(7) Jacobson, L. D.; Richard, R. M.; Lao, K. U.; Herbert, J. M. Efficient Monomer-Based Quantum Chemistry Methods for Molecular and Ionic Clusters. *Annu. Rep. Comput. Chem.* **2013**, *9*, 25−56.
(8) Lao, K. U.; Herbert, J. M. Accurate and Efficient Quantum Chemistry Calculations of Non-Covalent Interactions in Many-Body Systems: The XSAPT Family of Methods. *J. Phys. Chem. A* **2015**, *119*, 235−252.
(9) Barone, V.; Cossi, M.; Tomasi, J. A New Definition of Cavities for the Computation of Solvation Free Energies by the Polarizable Continuum Model. *J. Chem. Phys.* **1997**, *107*, 3210−3221.
(10) Herbert, J. M.; Lange, A. W. In *Many-Body Effects and Electrostatics in Multi-Scale Computations of Biomolecules*; Cui, Q., Ren, P., Meuwly, M., Eds.; Pan Stanford Publishing: Singapore, 2014.
(11) Cancés, E.; Mennucci, B.; Tomasi, J. A New Integral Equation Formalism for the Polarizable Continuum Model: Theoretical Background and Applications to Isotropic and Anisotropic Dielectrics. *J. Chem. Phys.* **1997**, *107*, 3032−3041.
(12) Tomasi, J.; Mennucci, B.; Cancès, E. The IEF Version of the PCM Solvation Method: An Overview of a New Method Addressed to Study Molecular Solutes at the QM Ab Initio Level. *J. Mol. Struct. (THEOCHEM)* **1999**, *464*, 211−226.
(13) Chipman, D. M. Charge Penetration in Dielectric Models of Solvation. *J. Chem. Phys.* **1997**, *106*, 10194−10206.
(14) Chipman, D. M. Reaction Field Treatment of Charge Penetration. *J. Chem. Phys.* **2000**, *112*, 5558−5565.
(15) Cancès, E.; Mennucci, B. Comment on "Reaction Field Treatment of Charge Penetration" [J. Chem. Phys. 112, 5558 (2000)]. *J. Chem. Phys.* **2001**, *114*, 4744−4745.
(16) Chipman, D. M. Comparison of Solvent Reaction Field Representations. *Theor. Chem. Acc.* **2002**, *107*, 80−89.
(17) Lange, A. W.; Herbert, J. M. Symmetric Versus Asymmetric Discretization of the Integral Equations in Polarizable Continuum Solvation Models. *Chem. Phys. Lett.* **2011**, *509*, 77−87.
(18) Shao, Y.; Gan, Z.; Epifanovsky, E.; Gilbert, A. T. B.; Wormit, M.; Kussmann, J.; Lange, A. W.; Behn, A.; Deng, J.; Feng, X.; et al. Advances in Molecular Quantum Chemistry Contained in the Q-Chem 4 Program Package. *Mol. Phys.* **2015**, *113*, 184−215.
(19) Lange, A. W.; Herbert, J. M. A Smooth, Non-Singular, and Faithful Discretization Scheme for Polarizable Continuum Models: The Switching Gaussian Approach. *J. Chem. Phys.* **2010**, *133*, 244111:1−18.
(20) You, Z.-Q.; Mewes, J.-M.; Dreuw, A.; Herbert, J. M. Comparison of the Marcus and Pekar partitions in the context of state-specific, non-equilibrium polarizable continuum models. Manuscript in preparation.
(21) Lunkenheimer, B.; Köhn, A. Solvent Effects on Electronically Excited States Using the Conductor-like Screening Model and the Second-Order Correlated Method ADC(2). *J. Chem. Theory Comput.* **2013**, *9*, 977−994.
(22) Cossi, M.; Barone, V. Separation Between Fast and Slow Polarizations in Continuum Solvation Models. *J. Phys. Chem. A* **2000**, *104*, 10614−10622.
(23) Klamt, A.; Schüürmann, G. COSMO: A New Approach to Dielectric Screening in Solvents with Explicit Expressions for the Screening Energy and Its Gradient. *J. Chem. Soc., Perkin Trans. 2* **1993**, 799−805.
(24) Dreuw, A.; Weisman, J. L.; Head-Gordon, M. Long-Range Charge-Transfer Excited States in Time-Dependent Density Functional Theory Require Non-Local Exchange. *J. Chem. Phys.* **2003**, *119*, 2943−2946.
(25) Dreuw, A.; Head-Gordon, M. Failure of Time-Dependent Density Functional Theory for Long-Range Charge-Transfer Excited-States: The Zincbacteriochlorin−Bacteriochlorin and Bacteriochlor-

DOI: 10.1021/jp511163y
J. Phys. Chem. A 2015, 119, 5446−5464

ophyll−Spheroidene Complexes. *J. Am. Chem. Soc.* **2004**, *126*, 4007−4016.
(26) Tawada, Y.; Tsuneda, T.; Yanagisawa, S.; Yanai, T.; Hirao, K. A Long-Range Corrected Time-Dependent Density Functional Theory. *J. Chem. Phys.* **2004**, *120*, 8425−8433.
(27) Rohrdanz, M. A.; Martins, K. M.; Herbert, J. M. A Long-Range-Corrected Density Functional That Performs Well for Both Ground-State Properties and Time-Dependent Density Functional Theory Excitation Energies, Including Charge-Transfer Excited States. *J. Chem. Phys.* **2009**, *130*, 054112:1−8.
(28) Stein, T.; Kronik, L.; Baer, R. Reliable Prediction of Charge Transfer Excitations in Molecular Complexes Using Time-Dependent Density Functional Theory. *J. Am. Chem. Soc.* **2009**, *131*, 2818−2820.
(29) Stein, T.; Kronik, L.; Baer, R. Prediction of Charge-Transfer Excitations in Coumarin-Based Dyes Using a Range-Separated Functional Tuned from First Principles. *J. Chem. Phys.* **2009**, *131*, 244119:1−5.
(30) Li, H.; Nieman, R.; Aquino, A. J. A.; Lischka, H.; Tretiak, S. Comparison of LC-TDDFT and ADC(2) Methods in Computations of Bright and Charge Transfer States in Stacked Oligothiophenes. *J. Chem. Theory Comput.* **2014**, *10*, 3280−3289.
(31) Olivares del Valle, F. J.; Tomasi, J. Electron Correlation and Solvation Effects. I. Basic Formulation and Preliminary Attempt to Include the Electron Correlation in the Quantum Mechanical Polarizable Continuum Model So As to Study Solvation Phenomena. *Chem. Phys.* **1991**, *150*, 139−150.
(32) Aguilar, M. A.; Olivares del Valle, F. J.; Tomasi, J. Electron Correlation and Solvation Effects. II. The Description of the Vibrational Properties of a Water Molecule in a Dielectric Given by the Application of the Polarizable Continuum Model with Inclusion of Correlation Effects. *Chem. Phys.* **1991**, *150*, 151−161.
(33) Olivares del Valle, F. J.; Bonaccorsi, R.; Cammi, R.; Tomasi, J. Electron Correlation and Solvation Effects: Part 3. Influence of the Basis Set and the Chemical Composition on the Solvation Energy Components Evaluated with the Quantum Mechanical Polarizable Continuum Model. *J. Mol. Struct. (THEOCHEM)* **1991**, *230*, 295−312.
(34) Ángyán, J. Choosing Between Alternative MP2 Algorithms in the Self-Consistent Reaction Field Theory of Solvent Effects. *Chem. Phys. Lett.* **1995**, *241*, 51−56.
(35) Karasulu, B.; Götze, J. P.; Thiel, W. Assessment of Franck−Condon Methods for Computing Vibrationally Broadened UV−vis Absorption Spectra of Flavin Derivatives: Riboflavin, Roseoflavin, and 5-Thioflavin. *J. Chem. Theory Comput.* **2014**, *10*, 5549−5566.
(36) Götze, J. P.; Karasulu, B.; Thiel, W. Computing UV/vis Spectra from the Adiabatic and Vertical Franck-Condon Schemes with the Use of Cartesian and Internal Coordinates. *J. Chem. Phys.* **2013**, *139*, −.
(37) Millefiori, S.; Favini, G.; Millefiori, A.; Grasso, D. Electronic Spectra and Structure of Nitroanilines. *Spectrochim. Acta, Part A* **1977**, *33*, 21−27.
(38) Millefiori, S.; Zuccarello, F.; Buemi, G. Excited State Dipole Moments of Nitrobenzene Derivatives. *J. Chem. Soc. Perkin Trans. 2* **1978**, 849−852.
(39) Buemi, G.; Millefiori, S.; Zuccarello, F.; Millefiori, A. Excited State Properties of Nitrobenzene Derivatives. *Can. J. Chem.* **1979**, *57*, 2167−2171.
(40) Zuccarello, F.; Millefiori, S.; Buemi, G. Electronic Spectra of Nitrobenzene Derivatives. *Spectrochim. Acta, Part A* **1979**, *35*, 223−227.
(41) Yomosa, S. Theory of the Excited State of Molecular Complex in Solution. *J. Phys. Soc. Jpn.* **1974**, *36*, 1655−1660.
(42) Klamt, A. Calculation of UV Vis Spectra in Solution. *J. Phys. Chem.* **1996**, *100*, 3349−3353.
(43) Caricato, M.; Mennucci, B.; Tomasi, J.; Ingrosso, F.; Cammi, R.; Corni, S.; Scalmani, G. Formation and Relaxation of Excited States in Solution: A New Time Dependent Polarizable Continuum Model Based on Time Dependent Density Functional Theory. *J. Chem. Phys.* **2006**, *124*, 124520.
(44) Chipman, D. M. Vertical Electronic Excitation with a Dielectric Continuum Model of Solvation Including Volume Polarization. I. Theory. *J. Chem. Phys.* **2009**, *131*, 014103:1−10.
(45) Schirmer, J. Beyond the Random-Phase Approximation: A New Approximation Scheme for the Polarization Propagator. *Phys. Rev. A* **1982**, *26*, 2395−2416.
(46) Dreuw, A.; Wormit, M. The Algebraic Diagrammatic Construction Scheme for the Polarization Propagator for the Calculation of Excited States. *Wiley Interdiscip. Rev.: Comput. Mol. Sci.* **2015**, *5*, 82−95.
(47) Jacobson, L. D.; Herbert, J. M. A Simple Algorithm for Determining Orthogonal, Self-Consistent Excited-State Wave Functions for a State-Specific Hamiltonian: Application to the Optical Spectrum of the Aqueous Electron. *J. Chem. Theory Comput.* **2011**, *7*, 2085−2093.
(48) Bottcher, C. J. F.; Belle, O. V.; Bordewijk, P.; Rip, A. *Theory of Electric Polarization; Dielectrics in Static Fields*; Elsevier: Amsterdam, 1973; Vol. *1*.
(49) Jacobson, L. D.; Williams, C. F.; Herbert, J. M. The Static-Exchange Electron-Water Pseudopotential, in Conjunction with a Polarizable Water Model: A New Hamiltonian for Hydrated-Electron Simulations. *J. Chem. Phys.* **2009**, *130*, 124115:1−18.
(50) Cammi, R.; Mennucci, B. Linear Response Theory for the Polarizable Continuum Model. *J. Chem. Phys.* **1999**, *110*, 9877−9886.
(51) Cammi, R.; Corni, S.; Mennucci, B.; Tomasi, J. Electronic Excitation Energies of Molecules in Solution: State Specific and Linear Response Methods for Nonequilibrium Continuum Solvation Models. *J. Chem. Phys.* **2005**, *122*, 104513:1−12.
(52) Gauss, J. In *Modern Methods and Algorithms of Quantum Chemistry*, 2nd ed.; Grotendorst, J., Ed.; NIC Series; John von Neumann Institute for Computing: Jülich, 2000; Vol. *3*, pp 541−592.
(53) Ronca, E.; Angeli, C.; Belpassi, L.; De Angelis, F.; Tarantelli, F.; Pastore, M. Density Relaxation in Time-Dependent Density Functional Theory: Combining Relaxed Density Natural Orbitals and Multireference Perturbation Theories for an Improved Description of Excited States. *J. Chem. Theory Comput.* **2014**, *10*, 4014−4024.
(54) Plasser, F.; Wormit, M.; Dreuw, A. New Tools for the Systematic Analysis and Visualization of Electronic Excitations. I. Formalism. *J. Chem. Phys.* **2014**, *140*, 024106:1−13.
(55) Plasser, F.; Bäppler, S. A.; Wormit, M.; Dreuw, A. New Tools for the Systematic Analysis and Visualization of Electronic Excitations. II. Applications. *J. Chem. Phys.* **2014**, *141*, 024107:1−12.
(56) Weigend, F.; Ahlrichs, R. Balanced Basis Sets of Split Valence, Triple Zeta Valence and Quadruple Zeta Valence Quality for H to Rn: Design and Assessment of Accuracy. *Phys. Chem. Chem. Phys.* **2005**, *7*, 3297−3305.
(57) Neese, F.; Schwabe, T.; Grimme, S. Analyic Derivatives for Perturbatively Corrected "double Hybrid" Density Functionals: Theory, Implementation, and Applications. *J. Chem. Phys.* **2007**, *126*, 124115.
(58) Grimme, S.; Antony, J.; Ehrlich, S.; Krieg, H. A Consistent and Accurate *ab Initio* Parameterization of Density Functional Dispersion Correction (DFT-D) for the 94 Elements H−Pu. *J. Chem. Phys.* **2010**, *132*, 154104:1−19.
(59) Klamt, A.; Jonas, V. Treatment of the Outlying Charge in Continuum Solvation Models. *J. Chem. Phys.* **1996**, *105*, 9972−9981.
(60) Neese, F. The ORCA Program System. *Wiley Interdiscip. Rev.: Comput. Mol. Sci.* **2012**, *2*, 73−78.
(61) Mewes, J.-M.; Jovanovic, V.; Marian, C. M.; Dreuw, A. On the Molecular Mechanism of Non-Radiative Decay of Nitrobenzene and the Unforeseen Challenges This Simple Molecule Holds for Electronic Structure Theory. *Phys. Chem. Chem. Phys.* **2014**, *16*, 12393−12406.
(62) Dunning, T. H., Jr. Gaussian Basis Sets for Use in Correlated Molecular Calculations. I. The Atoms Boron Through Neon and Hydrogen. *J. Chem. Phys.* **1989**, *90*, 1007−1023.
(63) Jacquemin, D.; Moore, B.; Planchat, A.; Adamo, C.; Autschbach, J. Performance of an Optimally Tuned Range-Separated Hybrid Functional for 0−0 Electronic Excitation Energies. *J. Chem. Theory Comput.* **2014**, *10*, 1677−1685.

DOI: 10.1021/jp511163y
J. Phys. Chem. A 2015, 119, 5446−5464

(64) Laurent, A. D.; Jacquemin, D. TD-DFT Benchmarks: A Review. *Int. J. Quantum Chem.* **2013**, *113*, 2019−2039.
(65) Stein, T.; Kronik, L.; Baer, R. Reliable Prediction of Charge Transfer Excitations in Molecular Complexes Using Time-Dependent Density Functional Theory. *J. Am. Chem. Soc.* **2009**, *131*, 2818−2820.
(66) Bondi, A. Van Der Waals Volumes and Radii. *J. Phys. Chem.* **1964**, *68*, 441−451.
(67) Rowland, R. S.; Taylor, R. Intermolecular Nonbonded Contact Distances in Organic Crystal Structures: Comparison with Distances Expected from Van Der Waals Radii. *J. Phys. Chem.* **1996**, *100*, 7384−7391.
(68) Kirketerp, M.-B. S.; Petersen, M. Å.; Wanko, M.; Leal, L. A. E.; Zettergren, H.; Raymo, F. M.; Rubio, A.; Nielsen, M. B.; Nielsen, S. B. Absorption Spectra of 4-Nitrophenolate Ions Measured *in Vacuo* and in Solution. *ChemPhysChem* **2009**, *10*, 1207−1209.
(69) Liu, J.; Liang, W. Analytical Second Derivatives of Excited-State Energy Within the Time-Dependent Density Functional Theory Coupled with a Conductor-like Polarizable Continuum Model. *J. Chem. Phys.* **2013**, *138*, 024101:1−10.
(70) Corni, S.; Cammi, R.; Mennucci, B.; Tomasi, J. Electronic Excitation Energies of Molecules in Solution Within Continuum Solvation Models: Investigating the Discrepancy Between State-Specific and Linear-Response Methods. *J. Chem. Phys.* **2005**, *123*, 134512:1−10.
(71) Schwabe, T.; Sneskov, K.; Olsen, J. M. H.; Kongsted, J.; Christiansen, O.; Hättig, C. PERI-CC2: A Polarizable Embedded RI-CC2Method. *J. Chem. Theory Comput.* **2012**, *8*, 3274−3283.

DOI: 10.1021/jp511163y
J. Phys. Chem. A 2015, 119, 5446−5464